a role in the stable transcriptional circuitry and in the rapid response upon the early differentiation of ESCs.

The current findings also suggest that Rest promotes the early ESC differentiation. Epiblast and the primitive endoderm are two distinct cell types in the inner cell mass (ICM) of the blastocyst. Genetic evidence indicates that the *Nanog* and *Gata* family transcription factors play a role in the segregation of epiblast and primitive endoderm within ICM (Chambers et al., 2003; Koutsourakis et al., 1999; Mitsui et al., 2003; Soudais et al., 1995). Indeed, Nanog and Gata6 are expressed in the ICM in a mutually exclusive manner (Chazaud et al., 2006), thus indicating the reciprocal control of the gene expression. The current study found that the conditional ablation of *Rest* results in the delayed repression of *Nanog* during the early differentiation of ESCs, whereas *REST* overexpression causes an increased expression of *Gata6*, which is accompanied by the rapid differentiation. In addition, the expression of *Fgf5*, an epiblast marker, was significantly downregulated by the *REST* overexpression. These results suggest that Rest may be involved in the segregation of epiblast and primitive endoderm through modifying the *Nanog* expression.

In summary, the conditional ablation of the *Rest* gene revealed that *Rest* is not absolutely required for the maintenance of ESC pluripotency. These results also indicate that *Rest* plays a role in the suppression of the pluripotent gene expression upon the early differentiation of ESCs.

SUPPLEMENTAL INFORMATION

Supplemental Information includes Supplemental Experimental Procedures and two figures and can be found with this article online at doi:10.1016/j.stem.2009.12.003.

ACKNOWLEDGMENTS

We would like to thank Hitoshi Niwa for helpful discussions, comments on the manuscript, and a plasmid expressing *EGFP-ires-Zeocin*. We would also like to thank HongQiang Sheng, Takeru Oyama, and Huilan Zhi for generating the *Rest* floxed ESCs. We thank Caroline Beard for a *Col1a-tetOP-cre* allele, Konrad Hochedlinger for a targeting plasmid containing *ires-GFP*, Kazutoshi Takahashi and Shinya Yamanaka for a *Nanog*-expressing plasmid, and Gail Mandel for a *REST*-expressing plasmid and a protocol for Rest western blot. We also thank Kyoko Takahashi, Ayako Suga, and Yoshitaka Kinjyo for their valuable technical assistance. This study was supported by grants from PRESTO, from the Ministry of Health, Labour and Welfare of Japan, from the Ministry of Education, Culture, Sports, Science and Technology of Japan, and from the Japan Science and Technology Agency (JST).

Received: September 2, 2009
Revised: November 11, 2009
Accepted: December 1, 2009
Published: January 7, 2010

REFERENCES

Andrés, M.E., Burger, C., Peral-Rubio, M.J., Battaglioli, E., Anderson, M.E., Grimes, J., Dallman, J., Ballas, N., and Mandel, G. (1999). CoREST: A functional corepressor required for regulation of neural-specific gene expression. Proc. Natl. Acad. Sci. USA *96*, 9873–9878.

Ballas, N., Grunseich, C., Lu, D.D., Speh, J.C., and Mandel, G. (2005). REST and its corepressors mediate plasticity of neuronal gene chromatin throughout neurogenesis. Cell *121*, 645–657.

Beard, C., Hochedlinger, K., Plath, K., Wutz, A., and Jaenisch, R. (2006). Efficient method to generate single-copy transgenic mice by site-specific integration in embryonic stem cells. Genesis *44*, 23–28.

Boyer, L.A., Lee, T.I., Cole, M.F., Johnstone, S.E., Levine, S.S., Zucker, J.P., Guenther, M.G., Kumar, R.M., Murray, H.L., Jenner, R.G., et al. (2005). Core transcriptional regulatory circuitry in human embryonic stem cells. Cell *122*, 947–956.

Boyer, L.A., Plath, K., Zeitlinger, J., Brambrink, T., Medeiros, L.A., Lee, T.I., Levine, S.S., Wernig, M., Tajonar, A., Ray, M.K., et al. (2006). Polycomb complexes repress developmental regulators in murine embryonic stem cells. Nature *441*, 349–353.

Buckley, N.J., Johnson, R., Sun, Y.M., and Stanton, L.W. (2009). Is REST a regulator of pluripotency? Nature *457*, E5–E6.

Chambers, I., Colby, D., Robertson, M., Nichols, J., Lee, S., Tweedie, S., and Smith, A. (2003). Functional expression cloning of Nanog, a pluripotency sustaining factor in embryonic stem cells. Cell *113*, 643–655.

Chazaud, C., Yamanaka, Y., Pawson, T., and Rossant, J. (2006). Early lineage segregation between epiblast and primitive endoderm in mouse blastocysts through the Grb2-MAPK pathway. Dev. Cell *10*, 615–624.

Chong, J.A., Tapia-Ramírez, J., Kim, S., Toledo-Aral, J.J., Zheng, Y., Boutros, M.C., Altshuller, Y.M., Frohman, M.A., Kraner, S.D., and Mandel, G. (1995). REST: A mammalian silencer protein that restricts sodium channel gene expression to neurons. Cell *80*, 949–957.

Fujikura, J., Yamato, E., Yonemura, S., Hosoda, K., Masui, S., Nakao, K., Miyazaki Ji, J., and Niwa, H. (2002). Differentiation of embryonic stem cells is induced by GATA factors. Genes Dev. *16*, 784–789.

Grimes, J.A., Nielsen, S.J., Battaglioli, E., Miska, E.A., Speh, J.C., Berry, D.L., Atouf, F., Holdener, B.C., Mandel, G., and Kouzarides, T. (2000). The co-repressor mSin3A is a functional component of the REST-CoREST repressor complex. J. Biol. Chem. *275*, 9461–9467.

Hochedlinger, K., Yamada, Y., Beard, C., and Jaenisch, R. (2005). Ectopic expression of Oct-4 blocks progenitor-cell differentiation and causes dysplasia in epithelial tissues. Cell *121*, 465–477.

Johnson, R., Teh, C.H., Kunarso, G., Wong, K.Y., Srinivasan, G., Cooper, M.L., Volta, M., Chan, S.S., Lipovich, L., Pollard, S.M., et al. (2008). REST regulates distinct transcriptional networks in embryonic and neural stem cells. PLoS Biol. *6*, e256.

Jørgensen, H.F., Chen, Z.F., Merkenschlager, M., and Fisher, A.G. (2009a). Is REST required for ESC pluripotency? Nature *457*, E4–E5.

Jørgensen, H.F., Terry, A., Beretta, C., Pereira, C.F., Leleu, M., Chen, Z.F., Kelly, C., Merkenschlager, M., and Fisher, A.G. (2009b). REST selectively represses a subset of RE1-containing neuronal genes in mouse embryonic stem cells. Development *136*, 715–721.

Koutsourakis, M., Langeveld, A., Patient, R., Beddington, R., and Grosveld, F. (1999). The transcription factor GATA6 is essential for early extra-embryonic development. Development *126*, 723–732.

Kunath, T., Saba-El-Leil, M.K., Almousailleakh, M., Wray, J., Meloche, S., and Smith, A. (2007). FGF stimulation of the Erk1/2 signalling cascade triggers transition of pluripotent embryonic stem cells from self-renewal to lineage commitment. Development *134*, 2895–2902.

Loh, Y.H., Wu, Q., Chew, J.L., Vega, V.B., Zhang, W., Chen, X., Bourque, G., George, J., Leong, B., Liu, J., et al. (2006). The Oct4 and Nanog transcription network regulates pluripotency in mouse embryonic stem cells. Nat. Genet. *38*, 431–440.

Mitsui, K., Tokuzawa, Y., Itoh, H., Segawa, K., Murakami, M., Takahashi, K., Maruyama, M., Maeda, M., and Yamanaka, S. (2003). The homeoprotein Nanog is required for maintenance of pluripotency in mouse epiblast and ES cells. Cell *113*, 631–642.

Niwa, H. (2007). How is pluripotency determined and maintained? Development *134*, 635–646.

Niwa, H., Miyazaki, J., and Smith, A.G. (2000). Quantitative expression of Oct-3/4 defines differentiation, dedifferentiation or self-renewal of ES cells. Nat. Genet. *24*, 372–376.

Schoenherr, C.J., and Anderson, D.J. (1995). The neuron-restrictive silencer factor (NRSF): A coordinate repressor of multiple neuron-specific genes. Science *267*, 1360–1363.

Schoenherr, C.J., Paquette, A.J., and Anderson, D.J. (1996). Identification of potential target genes for the neuron-restrictive silencer factor. Proc. Natl. Acad. Sci. USA *93*, 9881–9886.

Shimoda, M., Kanai-Azuma, M., Hara, K., Miyazaki, S., Kanai, Y., Monden, M., and Miyazaki, J. (2007). Sox17 plays a substantial role in late-stage differentiation of the extraembryonic endoderm in vitro. J. Cell Sci. *120*, 3859–3869.

Singh, S.K., Kagalwala, M.N., Parker-Thornburg, J., Adams, H., and Majumder, S. (2008). REST maintains self-renewal and pluripotency of embryonic stem cells. Nature *453*, 223–227.

Soudais, C., Bielinska, M., Heikinheimo, M., MacArthur, C.A., Narita, N., Saffitz, J.E., Simon, M.C., Leiden, J.M., and Wilson, D.B. (1995). Targeted mutagenesis of the transcription factor GATA-4 gene in mouse embryonic stem cells disrupts visceral endoderm differentiation in vitro. Development *121*, 3877–3888.

Sun, Y.M., Greenway, D.J., Johnson, R., Street, M., Belyaev, N.D., Deuchars, J., Bee, T., Wilde, S., and Buckley, N.J. (2005). Distinct profiles of REST interactions with its target genes at different stages of neuronal development. Mol. Biol. Cell *16*, 5630–5638.

Yamada, M., Onodera, M., Mizuno, Y., and Mochizuki, H. (2004). Neurogenesis in olfactory bulb identified by retroviral labeling in normal and 1-methyl-4-phenyl-1,2,3,6-tetrahydropyridine-treated adult mice. Neuroscience *124*, 173–181.

Yang, D.H., Smith, E.R., Roland, I.H., Sheng, Z., He, J., Martin, W.D., Hamilton, T.C., Lambeth, J.D., and Xu, X.X. (2002). Disabled-2 is essential for endodermal cell positioning and structure formation during mouse embryogenesis. Dev. Biol. *251*, 27–44.

Chemico-Biological Interactions 184 (2010) 423–430

Contents lists available at ScienceDirect

Chemico-Biological Interactions

journal homepage: www.elsevier.com/locate/chembioint

Genetic ablation of *Tnfα* demonstrates no detectable suppressive effect on inflammation-related mouse colon tumorigenesis

Hiroyasu Sakai[a,b], Yasuhiro Yamada[a,c,d,*], Masahito Shimizu[b], Kuniaki Saito[e], Hisataka Moriwaki[b], Akira Hara[a]

[a] Department of Tumor Pathology, Gifu University Graduate School of Medicine, 1-1 Yanagido, Gifu 501-1194, Japan
[b] Department of Medicine, Gifu University Graduate School of Medicine, 1-1 Yanagido, Gifu 501-1194, Japan
[c] PRESTO, Japan Science and Technology Agency, 4-1-8 Honcho Kawaguchi, Saitama, Japan
[d] Center for iPS Cell Research and Application (CiRA), Institute for Integrated Cell-material Sciences, Kyoto University, Kyoto 606-8507, Japan
[e] Human Health Science, Graduate School of Medicine and Faculty of Medicine, Kyoto University, 53 Kawahara-cho, Shogoin, Sakyo, Kyoto 606-8507, Japan

ARTICLE INFO

Article history:
Received 16 December 2009
Received in revised form 4 January 2010
Accepted 6 January 2010
Available online 14 January 2010

Keywords:
Tnfα
Inflammation-related colorectal cancer
Mouse

ABSTRACT

Colorectal cancer (CRC) is one of the most serious complications of inflammatory bowel disease. Tumor necrosis factor-α (Tnfα) is a major mediator of inflammation and there is increasing evidence that Tnfα/Tnf-receptor-1 (Tnfr1) signaling may act as an endogenous tumor promoter for colon carcinogenesis. In fact, a previous study revealed that mice lacking *Tnfr1* develop significantly fewer colonic tumors in the inflammation-related CRC model. In addition, antibodies against Tnfα have been shown to inhibit the development of inflammation-related CRC. In the present study, *Apc* Min/+; *Tnfα* −/− mice were treated with 2% dextran sodium sulfate (DSS) and the tumor development was compared with *Apc* Min/+; *Tnfα* +/+ control mice in order to investigate the role of Tnfα by itself in the inflammation-related CRC. Surprisingly, there were no detectable differences in either the severity of colonic inflammation or the expression of DSS-induced chemokines and cytokines (*Ccl2*, *Cxcl1*, *Tnfβ*, *Il1β*, *Il6*, and *Cox-2*) that relate to the colonic inflammation and tumorigenesis between these two groups. Furthermore, the genetic ablation of *Tnfα* did not suppress the colon tumorigenesis in comparison to the wild-type mice. Our observations suggest that intricate inflammatory responses promote the inflammation-related mouse colon tumorigenesis.

1. Introduction

The link between carcinogenesis and chronic inflammation has been recognized for certain types of cancer, including colorectal cancer (CRC) [1]. CRC is one of the serious complications of inflammatory bowel disease (IBD), including ulcerative colitis and Crohn's disease [1,2]. Although previous studies have demonstrated that the link between inflammation and CRC offers a possible strategy to prevent CRC, the underlying molecular processes involved in this interaction still remain poorly understood. Tumor necrosis factor-α (Tnfα) is a key cytokine involved in inflammation, immunity and cellular organization [3]. It was first isolated from the serum of mice infected with *Bacillus-Calmette–Guerin* treated with endotoxin, and shown to replicate the ability of endotoxin to induce haemorrhagic tumor necrosis [4]. Accordingly, it was originally utilized for the treatment of patients with advanced solid tumors [5]. In contrast, recent evidence indicates that Tnfα may act as an endogenous tumor promoter in several tumor tissues. Direct evidence for the involvement of Tnfα in malignancy came from observations that a genetic disruption of the *Tnfα* gene could significantly attenuate chemically induced skin tumor formation [6–8]. In addition, *Tnf-receptor-1* (*Tnfr1*) deficient mice had reduced oval cell (the putative hepatic stem cell) proliferation during the pre-neoplastic phase of liver carcinogenesis, correlating with fewer liver tumors than wild-type mice [9]. It has therefore been suggested that the Tnfα/Tnfr1 signaling pathway may play an important role in tumor promotion.

The predominant expression of Tnfα in colorectal cancer is observed within tumor-associated macrophages [10]. A previous study reported that Tnfα and Tnfr1 protein are expressed mainly in the infiltrating cells, such as macrophages and neutrophils which are derived from myeloid cells in inflamed colon tissue [11]. These infiltrating cells also express Cox-2 protein which is often up-regulated in colon carcinoma tissues and functionally promotes intestinal tumorigenesis [12]. Furthermore, Greten et al. reported that depleting *Ikkβ* in myeloid cells reduced the expression of pro-

Abbreviations: Tnfα, tumor necrosis factor-α; IBD, inflammatory bowel disease; Tnfr1, tumor necrosis factor-receptor-1; CRC, colorectal cancer; DSS, dextran sodium sulfate; Apc, adenomatous polyposis coli; Min, multiple intestinal neoplasia.

* Corresponding author at: Department of Tumor Pathology, Gifu University Graduate School of Medicine, 1-1 Yanagido, Gifu 501-1194, Japan. Tel.: +81 58 230 6225; fax: +81 58 230 6226.
E-mail addresses: y-yamada@cira.kyoto-u.ac.jp, y-yamada@gifu-u.ac.jp (Y. Yamada).

0009-2797/$ – see front matter © 2010 Elsevier Ireland Ltd. All rights reserved.
doi:10.1016/j.cbi.2010.01.014

inflammatory factor genes encoding Tnfα, Il1β, Il6, Kc, Cox-2 and Mmp-9 in the colon, followed by a suppression of colorectal tumor development in inflammation-related colon tumorigenesis [13].

It is noteworthy that the absence of *Tnfr1* significantly reduces the DSS-induced infiltration of Cox-2-expressing inflammatory cells, thus leading to a reduced incidence of colonic tumors [11]. Moreover, Tnfα can significantly increase Nf-kb activation in various cell types after binding to either Tnfr1 or Tnf-receptor-2 (Tnfr2) [14]. Therefore, it has been thought that endogenous Tnfα may activate Nf-kb signaling in inflammatory cells by interacting with Tnfr1 in an autocrine/paracrine manner and activated Nf-kb increases the expression of pro-inflammatory factors, which could thus lead to the promotion of colorectal tumorigenesis. Given the fact that Tnfr1 signaling is associated with tumorigenesis in the colon, Tnfα itself might be a therapeutic target for the inflammation-related mouse colon tumorigenesis. Indeed, previous studies demonstrated that antibodies against Tnfα inhibit the development of inflammation-related CRC [15].

Several animal models of experimental colitis have been developed for investigating the pathogenesis of IBD and IBD-related CRC and these are often used to evaluate new treatments for IBD [16]. Chemically induced models of intestinal inflammation, such as the dextran sodium sulfate (DSS)-induced model and the trinitrobenzene sulfonic acid (TNBS)-induced model, are the most generally used IBD animal models because the onset of inflammation is immediate and the procedure is relatively straightforward [17,18]. In contrast to the involvement of CD4+ T cells in TNBS-induced colitis, macrophages have been shown to play a central role in DSS-induced colitis [18,19]. Importantly, once *Apc* Min/+ mice, which harbor a germ line mutation in the *Apc* gene, are exposed to DSS, colitis markedly accelerates the development of dysplasia and cancer in the colon of *Apc* Min/+ mice [20]. Therefore, DSS-treated *Apc* Min/+ mouse can be useful for the investigation of inflammation-related colorectal tumorigenesis. The current study examined the effects of the genetic ablation of *Tnfα* on colon tumorigenesis using *Apc* Min/+; *Tnfα* −/− compound mutant mice exposed to DSS in order to determine whether Tnfα by itself could be a target for the prevention/treatment of inflammation-related colon tumorigenesis.

2. Materials and methods

2.1. Animals and diets

Apc Min/+ mice in the C57BL/6J background were obtained from The Jackson Laboratory (Bar Harbor, ME, USA). *Tnfα* −/− mice were maintained in C57BL/6J background [21]. We confirmed that the cell viability of splenocytes from *Tnfα* −/− mice is reduced after the stimulation with phorbol 12-myristate 13-acetate (PMA; 80 nM) and ionomycin (1 μM) when compared with that from *Tnfα* +/+ mice, thus suggesting the distinguishable responses against inflammatory stimuli between *Tnfα* +/+ and *Tnfα* −/− mice. Compound mutant *Apc* Min/+; *Tnfα* −/− mice were generated by breeding *Apc* Min/+; *Tnfα* +/− males to *Apc* +/+; *Tnfα* +/− females. These mice were maintained on a C57BL/6J genetic background to avoid potential strain differences in phenotype. All mice were bred and maintained in a specific pathogen-free animal facility under standard 12:12 h light:dark cycle and fed on a basal diet, CE-2 (CLEA Japan, Inc., Tokyo, Japan), and water *ad libitum* until the termination of the study.

2.2. Experimental procedures

DSS with a molecular weight of 36,000–50,000 (Wako, Osaka, Japan) was dissolved in distilled water at a concentration of 2% (w/v). Initially, 26 *Apc* Min/+; *Tnfα* +/+ mice (14 males and 12 females) and 25 *Apc* Min/+; *Tnfα* −/− mice (14 males and 11 females) were used for the macroscopic and histological study. The animals of these cohorts were given 2% (w/v) DSS in drinking water for 1 week, starting at 5 weeks of age, according to the protocol described in previous report [20]. The DSS-exposed *Apc* Min/+; *Tnfα* +/+ mice and *Apc* Min/+; *Tnfα* −/− mice were then sacrificed at 10 weeks of age for both the macroscopic inspection and histological analysis (Fig. 1a). Next, 20 male *Tnfα* +/+ mice and 19 male *Tnfα* −/− mice were treated with 2% (w/v) DSS in drinking water for 5 days, starting at 5 weeks of age, and then were sacrificed at day 0 (control, five mice in each group), day 10 (the acute phase of colonic inflammation, seven mice in each group) and day 30 (the chronic phase of colon inflammation, eight mice in *Tnfα* +/+ and seven mice in *Tnfα* −/−) after the exposure of DSS in order to compare the induction of pro-inflammatory factors in the presence or absence of *Tnfα* (Fig. 1b). Trinitrobenzene sulfonic acid (TNBS) was also used for another model of colonic inflammation. TNBS colitis was induced in five male *Tnfα* +/+ and six male *Tnfα* −/− mice according to the method of Wirtz et al. [18] with minor modifications. After the TNBS presensitization, the mice were lightly anesthetized, and an infant feeding catheter (3.5 Fr) was then carefully inserted into the colon such that the tip was 4 cm proximal to the anus. Five percent (w/v) in H_2O TNBS solution dissolved in the same volume of 100% ethanol was then slowly administered into the colon lumen through the catheter. The total injection volume was 100 μl in both groups, thus allowing TNBS to reach the entire colon. After the above administration, the mice were kept upside down while being held by their tails for 60 s and then were returned to their cages. All mice were then sacrificed at day 12 for both macroscopic inspection and histological analysis. At autopsy in each group of mice, their large bowel was flushed with saline, and then was excised. The large bowel from the ileocecal junction to the anal verge was measured, cut open longitudinally along the main axis, and then washed with saline. The total tumor number, tumor localization and the size of each tumor were recorded. The tumor volume was calculated as length × width × width × 0.526 [22]. After macroscopic inspection, it was rolled like a "*Swiss roll*" and then fixed overnight in 10% buffered formalin. Paraffin-embedded sections were made using routine procedures.

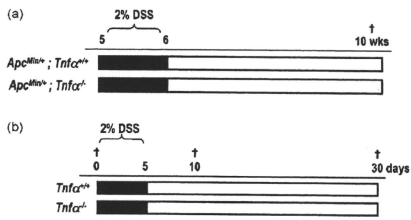

Fig. 1. Experimental protocols for this study. (a) Experimental design to investigate the role of Tnfα in DSS-induced colon tumorigenesis. (■) Basal diet and 2% DSS in drinking water, (□) basal diet and tap water, (↟) sacrifice. (b) Experimental design to compare the induction of pro-inflammatory factors in the presence or absence of *Tnfα*. Day 0, day 10 and day 30 represent control, the acute phase of colonic inflammation and the chronic phase of colon inflammation, respectively. (■) Basal diet and 2% DSS in drinking water, (□) basal diet and tap water, (↟) sacrifice.

2.3. Histological inflammation score

The histopathological alterations of the colon were examined on hematoxylin and eosin (H&E) stained sections and colon inflamma-

tion was scored according to the following morphological criteria as described previously [23]. Grade 0, normal colon mucosa; Grade 1, shortening and loss of the basal one-third of the actual crypts with mild inflammation and edema in the mucosa; Grade 2, loss of the basal two-thirds of the crypts with moderate inflammation in the mucosa; Grade 3, loss of all crypts with severe inflammation in the mucosa, but with retention of the surface epithelium; and Grade 4, loss of all crypts and surface epithelium with severe inflammation in the mucosa.

2.4. Immunohistochemical analysis

The avidin–biotin peroxidase complex technique was used for immunohistochemical studies. Sections (5 μm thick) were made, deparaffinized, rehydrated in PBS, placed in 10 mmol/l citrate buffer (pH 6.0), and heated in a 750 W microwave four times for 6 min. The endogenous peroxidase activity was blocked by incubation for 10 min in 0.3% H_2O_2. After washing three times with PBS, the sections were then preincubated with 2% bovine serum albumin in PBS for 40 min at room temperature and then incubated with primary antibodies, anti-β-catenin (1:1000; BD Biosciences PharMingen, San Diego, CA, USA), anti-Cox-2 (1:500; Santa Cruz Biotechnology, Santa Cruz, CA, USA) overnight at 4 °C. Subsequently, the sections were incubated with biotinylated secondary antibodies against the primary antibodies (1:250; DAKO Corp., Carpinteria, CA, USA) for 30 min followed by incubation with avidin-coupled peroxidase (Vector Laboratories, Inc., Burlingame, CA, USA) for 30 min at room temperature. The sections were developed with 3,3′-diaminobenzidine (DAB) using DAKO Liquid DAB Substrate-Chromogen System (DAKO) and then were counterstained with hematoxylin, dehydrated, and coverslipped.

2.5. Protein extraction and a Western blot analysis

Total protein was extracted from both the normal colon tissues and the colon tumor tissues, which were excised from *Apc* Min/+; *Tnfα* +/+ and *Apc* Min/+; *Tnfα* −/− mice at autopsy (Fig. 1a), and equivalent amounts of protein (15 μg/lane) were subjected to a Western blot analysis, as described previously [24,25]. The primary antibodies for β-catenin, GAPDH were purchased from BD Biosciences PharMingen (San Diego, CA, USA) and Cell Signaling Technology, Inc. (Danvers, MA, USA), respectively. An antibody against GAPDH served as a loading control.

2.6. Crypt isolation

The excised total colon was washed by PBS several times and cut opened in the longitudinal direction. The total colon was divided into three sections and the distal section was used for crypt isolation. The distal tissue was washed by 1× Hank's Balanced Salt Solution (HBSS; Sigma–Aldrich, St Louis, MO, USA) two times and followed by incubation with 1× HBSS containing 30 mM EDTA at 37 °C for 15 min. After this step, the tissue was dispersed by vortex in the 1× HBSS solution and separated into epithelial crypts and stromal tissues.

2.7. Quantitative real-time reversed transcription-polymerase chain reaction

Total RNA was extracted from the isolated epithelial crypts and stromal tissues of wild-type C57B6/J and Tnfα −/− mice at the indicated time intervals (Fig. 1b) by using the RNAqueous-4PCR kit (Ambion, Austin, TX, USA) according to the manufacturer's protocol. cDNA was synthesized from 1.0 μg of total RNA by using SuperScript III First-Strand Synthesis System (Invitrogen Life Technologies, Carlsbad, CA, USA). Quantitative real-time reverse transcription-polymerase chain reaction (qRT-PCR) amplification was performed in a final volume of 20 μl containing 10 μl of 2× SYBR green master mix (Takara, Kyoto, Japan), 1.0 μl of primers (10 μmol/l), 3.0 μl of distilled water and 5.0 μl of cDNA by using a LightCycler 1.0. (Roche Diagnostics, IN, USA) according to the protocols described previously [26]. The reaction conditions included activation at 95 °C for 10 min, denaturation at 95 °C for 10 s, annealing 60 °C for 10 s and extension 72 °C for 6 s. All PCR amplifications were done for 45 cycles. The expression level of each gene was normalized to the β-actin expression level using the standard curve method. The primer sequences used in qRT-PCR analyses were obtained from the PrimerBank (http://pga.mgh.harvard.edu/primerbank/): for *β-actin*, sense 5′-CATCCGTAAAGACCTCTATGCCAAC-3′ and antisense 5′-ATGGAGCCACCGATCCACA-3′; for *Tnfα*, sense 5′-CCCTCACACTCAGATCATCTTCT-3′ and antisense 5′-GCTACGACGTGGGCTACAG-3′; for *Tnfβ*, sense 5′-CCACCTCTTGAGGGTGCTTG-3′ and antisense 5′-CATGTCGGAGAAAGGCACGAT-3′; for *Ccl2*, sense 5′-TTAAAAACCTGGATCGGAACCAA-3′ and antisense 5′-GCATTAGCTTCAGATTTACGGGT-3′; for *Cxcl1*, sense 5′-CTGGGATTCACCTCAAGAACATC-3′ and antisense 5′-CAGGGTCAAGGCAAGCCTC-3′; for *Cox-2*, sense 5′-TGAGCAACTATTCCAAACCAGC-3′ and antisense 5′-GCACGTAGTCTTCGATCACTATC-3′; for *Il1β*, sense 5′-GCAACTGTTCCTGAACTCAACT-3′ and antisense 5′-ATCTTTTGGGGTCCGTCAACT-3′; and for *Il6*, sense 5′-TAGTCCTTCCTACCCCAATTTCC-3′ and antisense 5′-TTGGTCCTTAGCCACTCCTTC-3′.

2.8. Statistical analysis

The statistical analysis was performed using the GraphPad Prism 4 software program (Graphpad Software, Inc., San Diego, CA, USA). The mean ± SD was calculated for all parameters determined. Statistical significance was evaluated using either Student's *t*-test or Welch's *t*-test for paired samples. *p* values <0.05 were considered to be statistically significant.

3. Results

3.1. Genetic ablation of Tnfα did not suppress both the colonic inflammation and the expression of pro-inflammatory factors in the colon of mice exposed to DSS

A previous study revealed that *Tnfr1* deficient mice are resistant to the DSS-induced colitis. In the present study, two cohorts of *Apc* Min/+ mice with different *Tnfα* status (*Apc* Min/+; *Tnfα* +/+, *Apc* Min/+; *Tnfα* −/− mice) were exposed to 2% DSS in drinking water for 1 week and sacrificed at the point of week 5 (Fig. 1a). In contrast to the *Tnfr1* deficient mice, mice lacking *Tnfα*, as well as the control mice, exhibited profound body weight loss and bloody diarrhea during the course of DSS treatment. In addition, there were no significant differences in either the physical findings or mortality between *Apc* Min/+; *Tnfα* +/+ and *Apc* Min/+; *Tnfα* −/− mice. There were no apparent differences in either microscopic appearance of the inflamed colon (data not shown) or the histological inflammation score (1.17 ± 0.83 and 1.25 ± 0.97, respectively, *p*: 0.82) between these two cohorts.

We also examined the effect of *Tnfα* ablation on intestinal inflammation using the trinitrobenzene sulfonic acid (TNBS)-induced model, a different model of intestinal inflammation. However, we could not detect any differences in the histological inflammation score between *Tnfα* +/+ and *Tnfα* −/− mice (2.75 ± 1.50 and 2.50 ± 1.22, respectively, *p*: 0.78).

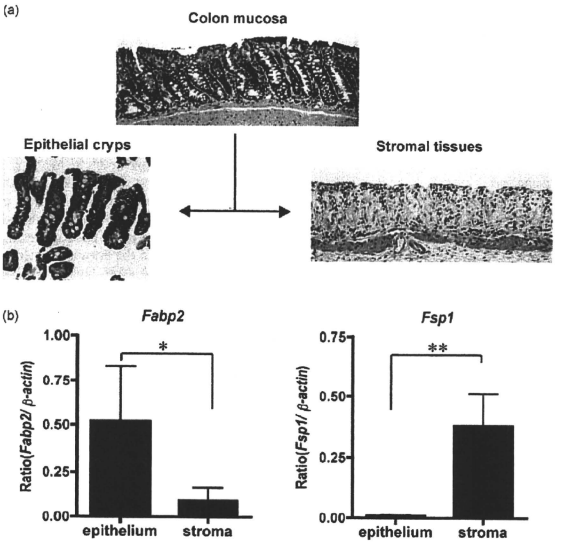

Fig. 2. Crypt isolation and the expression of epithelial or stromal marker gene. (a) Distal colon tissues were separated into epithelial crypts and stromal tissues by crypt isolation as described in Section 2. (b) Quantitative RT-PCR was performed on total RNAs extracted from both epithelial cryps and stromal tissues. The levels of FABP2 and FSP-1 mRNA were normalized to β-actin mRNA levels. Representative results from three independent experiments are shown here. Data represent the mean ± SD. Statistical significance of differences was evaluated by Student's *t*-test with Welch's correction. $^{*}p < 0.05$, $^{**}p < 0.01$.

Both wild-type and *Tnfα* deficient mice were treated with 2% DSS for 5 days and then were sacrificed at day 0 (control), day 10 (the acute phase of colonic inflammation) and day 30 (the chronic phase of colon inflammation; Fig. 1b) in order to compare the induction of pro-inflammatory factors in the presence or absence of *Tnfα*. The crypts were isolated to separate the colons into the epithelial crypts and stromal tissues (Fig. 2a). After crypt isolation, RNA was extracted from these tissue specimens and real-time PCR was used to compare the expression of pro-inflammatory factors between wild-type and *Tnfα* deficient mice. The epithelial marker, *fatty-acid-binding-protein-2* (*Fabp2*) [27–29], was predominantly expressed by RNAs from colonic crypts, whereas the mesenchymal marker, *fibroblast-specific-protein-1* (*Fsp1*), was predominantly expressed at those from stromal tissues (Fig. 2b). These findings indicate that epithelial cells were therefore successfully separated from stromal cells.

The expression of pro-inflammatory factors (*Tnfα*, *Tnfβ*, *Ccl2*, *Cxcl1*, *Il1β*, *Il6*, *Cox-2*) were up-regulated after the DSS exposure in wild-type mice and such altered expression was maintained at a high level until day 30 (Fig. 3a). As expected, during the course of DSS treatment (Fig. 1b), the expression of *Tnfα* was not detectable in either the epithelial or stromal tissues of *Tnfα* deficient mice (Fig. 3b). However, in spite of the lack of *Tnfα* expression, there were no significant differences in the expression of *Tnfβ*, *Ccl2*, *Cxcl1*, *Il1β*, *Il6* and *Cox-2* in either the epithelial or stromal tissues between the wild-type and *Tnfα* deficient mice (Fig. 3c). These results indicate that the genetic ablation of *Tnfα* did not influence either the severity of colitis or the expression of DSS-induced pro-inflammatory factors.

3.2. Genetic ablation of *Tnfα* did not suppress the infiltration of Cox-2-expressing inflammatory cells and the accumulation of β-catenin protein in the inflamed colorectal tumor tissues

The coordinated activation of the Apc/β-catenin pathway and the Cox-2 signaling pathway plays an important role in colon tumor formation and progression [30]. A previous study revealed a lack of *Tnfr1* to lead to the decreased expression of Cox-2 in the stromal tissues and the decreased expression of nuclear β-catenin in the colonic tumor cells [11]. Therefore, the infiltration of Cox-2-expressing inflammatory cells and the accumulation of nuclear β-catenin was examined by immunostaining. In contrast to previous data, no significant differences were observed in the infiltration index of Cox-2-positive inflammatory cells between *Apc* Min/+; *Tnfα* +/+ and *Apc* Min/+; *Tnfα* −/− mice (42.62 ± 6.65 and 45.73 ± 2.90 cells per field at 400× magnification, respectively, *p*: 0.32) (Fig. 4a). The accumulation of nuclear β-catenin protein in colon tumor cells was not different between the two cohorts (Fig. 4b). In addition, Western blotting revealed the expression of β-catenin protein in colonic tumors to not change between *Apc* Min/+; *Tnfα* +/+ and *Apc* Min/+; *Tnfα* −/− mice (Fig. 4c).

3.3. The genetic ablation of *Tnfα* did not suppress the inflammation-related colon tumorigenesis

Tnfr1 deficient mice markedly attenuate tumor formation induced by azoxymethane (AOM) and DSS in comparison to wild-type mice [11]. In the present study, as in a previous report [20], colon tumors were detectable only in *Apc* Min/+ mice exposed to

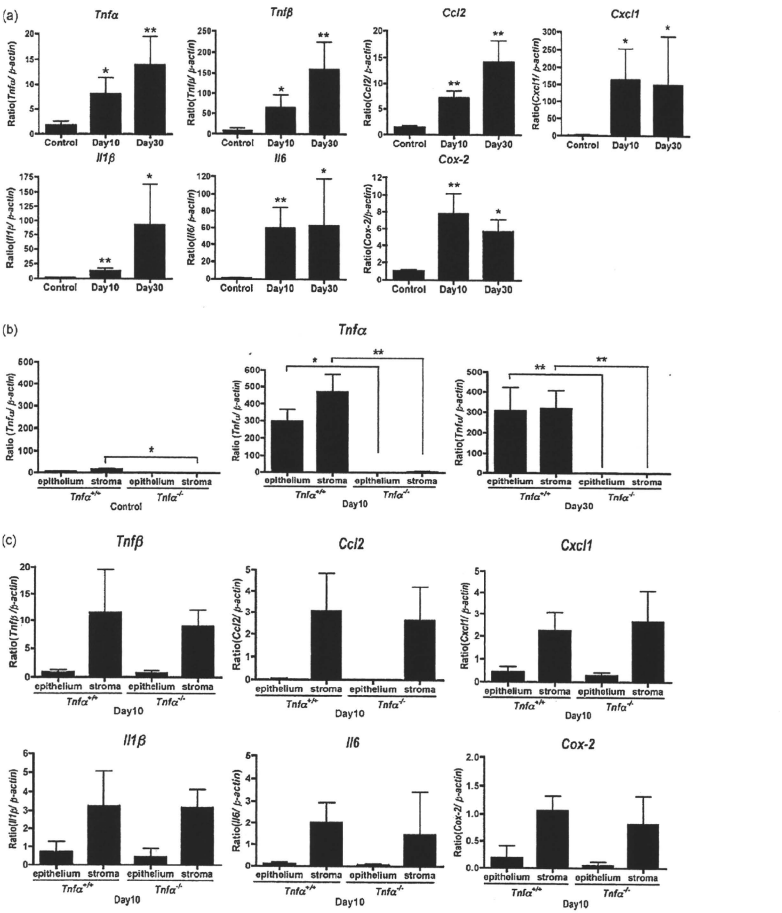

Fig. 3. Pro-inflammatory factor gene expression in the colon. Quantitative RT-PCR was performed on total RNAs extracted from stromal tissues of wild-type mice (a), epithelial and stromal tissues of both wild-type and Tnfα$^{-/-}$ mice (b and c) at the indicated time intervals as indicated. The levels of each pro-inflammatory factor were normalized to β-actin mRNA levels. Representative results from three independent experiments are shown here. Data represent the mean ± SD. Statistical significance of differences was evaluated by Student's *t*-test with Welch's correction (a–c). $^{*}p < 0.05$, $^{**}p < 0.01$.

DSS, whereas no tumors were found in *Apc* +/+ mice with the DSS exposure. The incidence and multiplicity of colonic tumors were 100% and 16.15 ± 5.84/mouse in *Apc* Min/+; *Tnfα* +/+ mice and 100% and 14.27 ± 7.71/mouse in *Apc* Min/+; *Tnfα* −/− mice, respectively. The tumor volumes were 3.90 ± 2.55 mm^3 and 3.81 ± 2.49 mm^3 in *Apc* Min/+; *Tnfα* +/+ and *Apc* Min/+; *Tnfα* −/− mice, respectively (Table 1). Importantly, no significant differences were observed in either the tumor incidence and multiplicity or the tumor volumes between *Apc* Min/+; *Tnfα*+/+ and *Apc* Min/+; *Tnfα*−/− mice. Microscopic examinations also failed to detect any histological differences in colon tumors between *Apc* Min/+; *Tnfα* +/+ and *Apc* Min/+; *Tnfα* −/− mice (data not shown). In addition, the incidence and multiplicity of small intestinal tumors did not alter regardless of the *Tnfα* status (100% and 47.0 ± 2.16/mouse in *Apc* Min/+; *Tnfα* +/+ mice and 100% and 48.8 ± 3.59/mouse in *Apc* Min/+; *Tnfα* −/− mice, respectively).

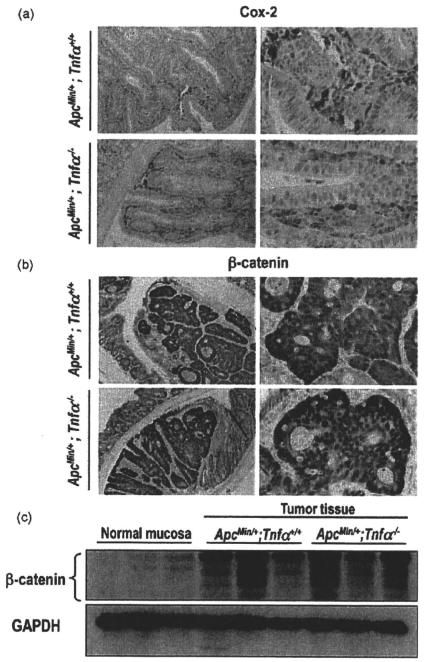

Fig. 4. Cox-2-expressing cells and β-catenin nuclear accumulation in the colon tumor tissues. Colons were immunostained with anti-Cox-2 (a) or anti-β-catenin antibody (b) and representative results from five independent animals are shown here. Original magnification, 100× (left panels), 400× (right panels), respectively. (c) Western blot analysis with anti-β-catenin antibody was performed on cell lysates from both normal colon mucosa and colon tumor tissues. Representative results from three independent experiments are shown here.

4. Discussion

Tnfα is a hormone with a broad spectrum of biological activities, produced mainly by activated macrophages and a variety of other cell types, including activated T cells, mast cells, neutrophils, and astrocytes [31]. Once the protein is efficiently exported from the producing cell, it enters the circulation, where it has a very limited half-life and binds to either high-affinity 55-kDa TNF-receptor-1 (Tnfr1) or low-affinity 75-kDa TNF-receptor-2 (Tnfr2) [32,33]. Popivanova et al. revealed that mice lacking *Tnfr*1 treated with AOM and DSS showed reduced mucosal damage, reduced infiltration of macrophages and neutrophils, and attenuated subsequent tumor formation [11]. These findings indicate Tnfα/Tnfr1 signaling as a crucial mediator of the initiation and promotion of colitis-associated colon carcinogenesis, and suggest that targeting Tnfα may be a useful strategy for prevention and/or treatment of colon cancer in the individuals with IBD.

Table 1
Incidence, multiplicity and tumor volume of large intestinal tumors at week 5.

Genotype	Incidence	Multiplicity[a]	Tumor volume[b]
$Apc^{Min/+}$; $Tnf\alpha^{+/+}$	26/26, 100%	16.15 ± 5.84	3.90 ± 2.25
$Apc^{Min/+}$; $Tnf\alpha^{-/-}$	25/25, 100%	14.27 ± 7.71	3.81 ± 2.49

Statistical significance of differences was evaluated by Student's *t*-test.
[a] Number of tumors/mouse, the mean ± SD.
[b] Tumor volume was calculated as length × width × width × 0.526, the mean ± SD.

In contrast [11], the current study revealed that, despite a deficiency in the *Tnfα* expression, both chemically induced colonic inflammation and the tumor formation in *Tnfα* deficient mice were not attenuated in comparison to those of *Tnfα* +/+ control mice. In addition, the expression of pro-inflammatory factors in the colon mucosa exposed to DSS was not altered in comparison to wild-type control mice. Moreover, no significant differences were observed in either the infiltration of Cox-2-positive inflammatory cells or the nuclear β-catenin accumulation of tumor cells between *Apc* Min/+:*Tnfα* +/+ and *Apc* Min/+:*Tnfα* −/− mice, both of which have been shown to be significantly suppressed in *Tnfr*1 deficient mice [11].

Although Tnfα is the ligand for the Tnfr1, it is noteworthy that Tnfr1 also binds with tumor necrosis factor-β (Tnfβ) or lymphotoxin (LT) [34]. Tnfβ shares about 30% structural homology with Tnfα [35,36], and Tnfα and Tnfβ are functionally indistinguishable with respect to receptor binding and activation of Nf-kB in HL60 cells [37]. Although DSS-induced *Tnfβ* expression was almost equal in both wild-type and *Tnfα* deficient mice, it might be possible that Tnfβ is involved in the induction of colonic inflammation and inflammation-related colon tumorigenesis induced by DSS. This finding is consistent with the previous findings that activation of Nf-kB is associated with DSS-induced inflammation-related colon tumorigenesis [13,38] and that the maximum activation of Nf-kB with Tnfα and/or Tnfβ requires only a small fraction of the total number of Tnf-receptors to be occupied [39].

Previous studies demonstrated that several inflammation-related factors including *Il*1β, Stat3 and iNOS are involved in DSS-induced inflammation-related colon tumorigenesis [38,40,41]. In addition, the possible interaction between iNOS, TnFα and *Il*1β is suggested to play a role in the tumor promotion of inflammation-related colon carcinogenesis [42]. Given such intricate inflammatory responses, it is also possible that the Tnfα-independent signal may promote the inflammation-related mouse colon tumorigenesis in the present study.

There is increasing evidence that the anti-Tnfα monoclonal antibody, infliximab, is an effective therapy for IBD, including Crohn's disease and ulcerative colitis [43–49]. Infliximab is a chimeric monoclonal antibody that binds not only the soluble subunit of Tnfα but also the membrane-bound precursor of Tnfα [50,51]. Infliximab inhibits a broad range of biological activities of Tnfα by blocking the interaction of Tnfα with its receptors. Given the fact that the genetic deletion for *Tnfr*1 significantly suppressed inflammation-related colon tumorigenesis, it was expected that the blockage for Tnfα with the use of infliximab could be a useful strategy for both the chemoprevention and therapy for tumorigenesis. Indeed, previous studies demonstrated that antibodies against Tnfα strongly suppress the development of inflammation-related CRC [11,15]. In contrast, the current study revealed that the genetic ablation of Tnfα alone did not either reduce colon inflammation or attenuate tumor formation. Our results may therefore suggest that an indirect action of anti-Tnfα antibodies exerts a tumor suppressive effect in inflammation-related CRC. A previous study demonstrated that anti-Tnfα monoclonal antibody binds to the transmembrane form of Tnfα, thus resulting in the efficient killing of the Tnfα-expressing cells by both antibody-dependent cellular toxicity and complement-dependent cytotoxicity effector mechanisms [51,52]. The mode of action of anti-Tnfα monoclonal antibody for the treatment of IBD and IBD-related tumorigenesis might be attributed principally to the lysis of the inflammatory

cells rather than blocking the interaction of Tnfα with its receptors.

In conclusion, the current study revealed that the genetic ablation of *Tnfα* results in no detectable effect on either the suppression of DSS-induced colonic inflammation or the attenuation of inflammation-related mouse colon tumorigenesis. These observations suggest that intricate inflammatory responses are involved in the inflammation-related mouse colon tumorigenesis.

Conflicts of interest

No conflicts of interest.

Acknowledgments

We would like to thank Kyoko Takahashi, Ayako Suga, and Yoshitaka Kinjyo for their valuable technical assistance and animal care. This study was supported by grants from Japan Science and Technology (JST), grants from PRESTO, grants from the Ministry of Health, Labour and Welfare of Japan, and grants from the Ministry of Education, Culture, Sports, Science and Technology of Japan.

References

[1] S.P. Hussain, L.J. Hofseth, C.C. Harris, Radical causes of cancer, Nat. Rev. Cancer 3 (4) (2003) 276–285.
[2] B.A. Lashner, K.S. Provencher, J.M. Bozdech, A. Brzezinski, Worsening risk for the development of dysplasia or cancer in patients with chronic ulcerative colitis, Am. J. Gastroenterol. 90 (3) (1995) 377–380.
[3] R.M. Locksley, N. Killeen, M.J. Lenardo, The TNF and TNF receptor superfamilies: integrating mammalian biology, Cell 104 (4) (2001) 487–501.
[4] E.A. Carswell, L.J. Old, R.L. Kassel, S. Green, N. Fiore, B. Williamson, An endotoxin-induced serum factor that causes necrosis of tumors, Proc. Natl. Acad. Sci. U.S.A. 72 (9) (1975) 3666–3670.
[5] N. Senzer, S. Mani, A. Rosemurgy, J. Nemunaitis, C. Cunningham, C. Guha, N. Bayol, M. Gillen, K. Chu, C. Rasmussen, H. Rasmussen, D. Kufe, R. Weichselbaum, N. Hanna, TNFerade biologic, an adenovector with a radiation-inducible promoter, carrying the human tumor necrosis factor alpha gene: a phase I study in patients with solid tumors, J. Clin. Oncol. 22 (4) (2004) 592–601.
[6] R.J. Moore, D.M. Owens, G. Stamp, C. Arnott, F. Burke, N. East, H. Holdsworth, L. Turner, B. Rollins, M. Pasparakis, G. Kollias, F. Balkwill, Mice deficient in tumor necrosis factor-alpha are resistant to skin carcinogenesis, Nat. Med. 5 (7) (1999) 828–831.
[7] M. Suganuma, S. Okabe, M.W. Marino, A. Sakai, E. Sueoka, H. Fujiki, Essential role of tumor necrosis factor alpha (TNF-alpha) in tumor promotion as revealed by TNF-alpha-deficient mice, Cancer Res. 59 (18) (1999) 4516–4518.
[8] K.A. Scott, R.J. Moore, C.H. Arnott, N. East, R.G. Thompson, B.J. Scallon, D.J. Shealy, F.R. Balkwill, An anti-tumor necrosis factor-alpha antibody inhibits the development of experimental skin tumors, Mol. Cancer Ther. 2 (5) (2003) 445–451.
[9] B. Knight, G.C. Yeoh, K.L. Husk, T. Ly, L.J. Abraham, C. Yu, J.A. Rhim, N. Fausto, Impaired preneoplastic changes and liver tumor formation in tumor necrosis factor receptor type 1 knockout mice, J. Exp. Med. 192 (12) (2000) 1809–1818.
[10] M.S. Naylor, G.W. Stamp, F.R. Balkwill, Investigation of cytokine gene expression in human colorectal cancer, Cancer Res. 50 (14) (1990) 4436–4440.
[11] B.K. Popivanova, K. Kitamura, Y. Wu, T. Kondo, T. Kagaya, S. Kaneko, M. Oshima, C. Fujii, N. Mukaida, Blocking TNF-alpha in mice reduces colorectal carcinogenesis associated with chronic colitis, J. Clin. Invest. 118 (2) (2008) 560–570.
[12] H. Sano, Y. Kawahito, R.L. Wilder, A. Hashiramoto, S. Mukai, K. Asai, S. Kimura, H. Kato, M. Kondo, T. Hla, Expression of cyclooxygenase-1 and -2 in human colorectal cancer, Cancer Res. 55 (17) (1995) 3785–3789.
[13] F.R. Greten, L. Eckmann, T.F. Greten, J.M. Park, Z.W. Li, L.J. Egan, M.F. Kagnoff, M. Karin, IKKbeta links inflammation and tumorigenesis in a mouse model of colitis-associated cancer, Cell 118 (3) (2004) 285–296.
[14] Q. Li, S. Withoff, I.M. Verma, Inflammation-associated cancer: NF-kappaB is the lynchpin, Trends Immunol. 26 (6) (2005) 318–325.
[15] M. Onizawa, T. Nagaishi, T. Kanai, K. Nagano, S. Oshima, Y. Nemoto, A. Yoshioka, T. Totsuka, R. Okamoto, T. Nakamura, N. Sakamoto, K. Tsuchiya, K. Aoki, K. Ohya, H. Yagita, M. Watanabe, Signaling pathway via TNF-alpha/NF-kappaB in intestinal epithelial cells may be directly involved in colitis-associated carcinogenesis, Am. J. Physiol. Gastrointest. Liver Physiol. 296 (4) (2009) G850–859.
[16] S.H. Itzkowitz, X. Yio, Inflammation and cancer IV. Colorectal cancer in inflammatory bowel disease: the role of inflammation, Am. J. Physiol. Gastrointest. Liver Physiol. 287 (1) (2004) G7–17.
[17] M. Kawada, A. Arihiro, E. Mizoguchi, Insights from advances in research of chemically induced experimental models of human inflammatory bowel disease, World J. Gastroenterol. 13 (42) (2007) 5581–5593.
[18] S. Wirtz, C. Neufert, B. Weigmann, M.F. Neurath, Chemically induced mouse models of intestinal inflammation, Nat. Protoc. 2 (3) (2007) 541–546.
[19] L.A. Dieleman, B.U. Ridwan, G.S. Tennyson, K.W. Beagley, R.P. Bucy, C.O. Elson, Dextran sulfate sodium-induced colitis occurs in severe combined immunodeficient mice, Gastroenterology 107 (6) (1994) 1643–1652.
[20] T. Tanaka, H. Kohno, R. Suzuki, K. Hata, S. Sugie, N. Niho, K. Sakano, M. Takahashi, K. Wakabayashi, Dextran sodium sulfate strongly promotes colorectal carcinogenesis in Apc(Min/+) mice: inflammatory stimuli by dextran sodium sulfate results in development of multiple colonic neoplasms, Int. J. Cancer 118 (1) (2006) 25–34.
[21] T. Taniguchi, M. Takata, A. Ikeda, E. Momotani, K. Sekikawa, Failure of germinal center formation and impairment of response to endotoxin in tumor necrosis factor alpha-deficient mice, Lab. Invest. 77 (6) (1997) 647–658.
[22] N.R. Murray, J. Weems, U. Braun, M. Leitges, A.P. Fields, Protein kinase C betaII and PKCiota/lambda: collaborating partners in colon cancer promotion and progression, Cancer Res. 69 (2) (2009) 656–662.
[23] H.S. Cooper, S.N. Murthy, R.S. Shah, D.J. Sedergran, Clinicopathologic study of dextran sulfate sodium experimental murine colitis, Lab. Invest. 69 (2) (1993) 238–249.
[24] M. Shimizu, A. Deguchi, Y. Hara, H. Moriwaki, I.B. Weinstein, EGCG inhibits activation of the insulin-like growth factor-1 receptor in human colon cancer cells, Biochem. Biophys. Res. Commun. 334 (3) (2005) 947–953.
[25] M. Shimizu, A. Deguchi, A.K. Joe, J.F. McKoy, H. Moriwaki, I.B. Weinstein, EGCG inhibits activation of HER3 and expression of cyclooxygenase-2 in human colon cancer cells, J. Exp. Ther. Oncol. 5 (1) (2005) 69–78.
[26] T. Oyama, Y. Yamada, K. Hata, H. Tomita, A. Hirata, H. Sheng, A. Hara, H. Aoki, T. Kunisada, S. Yamashita, H. Mori, Further upregulation of beta-catenin/Tcf transcription is involved in the development of macroscopic tumors in the colon of ApcMin/+ mice, Carcinogenesis 29 (3) (2008) 666–672.
[27] H.M. Shields, M.L. Bates, N.M. Bass, C.J. Best, D.H. Alpers, R.K. Ockner, Light microscopic immunocytochemical localization of hepatic and intestinal types of fatty acid-binding proteins in rat small intestine, J. Lipid Res. 27 (5) (1986) 549–557.
[28] D.A. Sweetser, S.M. Hauft, P.C. Hoppe, E.H. Birkenmeier, J.I. Gordon, Transgenic mice containing intestinal fatty acid-binding protein–human growth hormone fusion genes exhibit correct regional and cell-specific expression of the reporter gene in their small intestine, Proc. Natl. Acad. Sci. U.S.A. 85 (24) (1988) 9611–9615.
[29] A. Haegebarth, W. Bie, R. Yang, S.E. Crawford, V. Vasioukhin, E. Fuchs, A.L. Tyner, Protein tyrosine kinase 6 negatively regulates growth and promotes enterocyte differentiation in the small intestine, Mol. Cell. Biol. 26 (13) (2006) 4949–4957.
[30] M. Oshima, J.E. Dinchuk, S.L. Kargman, H. Oshima, B. Hancock, E. Kwong, J.M. Trzaskos, J.F. Evans, M.M. Taketo, Suppression of intestinal polyposis in Apc delta716 knockout mice by inhibition of cyclooxygenase 2 (COX-2), Cell 87 (5) (1996) 803–809.
[31] P.W. Szlosarek, F.R. Balkwill, Tumour necrosis factor alpha: a potential target for the therapy of solid tumours, Lancet Oncol. 4 (9) (2003) 565–573.
[32] B.A. Beutler, I.W. Milsark, A. Cerami, Cachectin/tumor necrosis factor: production, distribution, and metabolic fate in vivo, J. Immunol. 135 (6) (1985) 3972–3977.
[33] S. de Kossodo, G.E. Grau, J.A. Louis, I. Muller, Tumor necrosis factor alpha (TNF-alpha) and TNF-beta and their receptors in experimental cutaneous leishmaniasis, Infect. Immun. 62 (4) (1994) 1414–1420.
[34] L.A. Tartaglia, D.V. Goeddel, Two TNF receptors, Immunol. Today 13 (5) (1992) 151–153.
[35] M.J. Eck, M. Ultsch, E. Rinderknecht, A.M. de Vos, S.R. Sprang, The structure of human lymphotoxin (tumor necrosis factor-beta) at 1.9-A resolution, J. Biol. Chem. 267 (4) (1992) 2119–2122.
[36] J. Browning, A. Ribolini, Studies on the differing effects of tumor necrosis factor and lymphotoxin on the growth of several human tumor lines, J. Immunol. 143 (6) (1989) 1859–1867. .
[37] H.P. Hohmann, R. Kolbeck, R. Remy, A.P. van Loon, Cyclic AMP-independent activation of transcription factor NF-kappa B in HL60 cells by tumor necrosis factors alpha and beta, Mol. Cell. Biol. 11 (4) (1991) 2315–2318.
[38] M. Kim, S. Miyamoto, Y. Yasui, T. Oyama, A. Murakami, T. Tanaka, Zerumbone, a tropical ginger sesquiterpene, inhibits colon and lung carcinogenesis in mice, Int. J. Cancer 124 (2) (2009) 264–271.
[39] M.M. Chaturvedi, M. Higuchi, B.B. Aggarwal, Effect of tumor necrosis factors, interferons, interleukins, and growth factors on the activation of NF-kappa B: evidence for lack of correlation with cell proliferation, Lymphokine Cytokine Res. 13 (5) (1994) 309–313.
[40] T. Tanaka, R. Suzuki, H. Kohno, S. Sugie, M. Takahashi, K. Wakabayashi, Colonic adenocarcinomas rapidly induced by the combined treatment with 2-amino-1-methyl-6-phenylimidazo[4,5-b]pyridine and dextran sodium sulfate in male ICR mice possess beta-catenin gene mutations and increases immunoreactivity for beta-catenin, cyclooxygenase-2 and inducible nitric oxide synthase, Carcinogenesis 26 (1) (2005) 229–238.
[41] T. Tanaka, Y. Yasui, M. Tanaka, T. Oyama, K.M. Rahman, Melatonin suppresses AOM/DSS-induced large bowel oncogenesis in rats, Chem. Biol. Interact. 177 (2) (2009) 128–136.
[42] H. Kohno, M. Takahashi, Y. Yasui, R. Suzuki, S. Miyamoto, Y. Kamanaka, M. Naka, T. Maruyama, K. Wakabayashi, T. Tanaka, A specific inducible nitric oxide synthase inhibitor, ONO-1714 attenuates inflammation-related large bowel carcinogenesis in male Apc(Min/+) mice, Int. J. Cancer 121 (3) (2007) 506–513.
[43] D.H. Present, P. Rutgeerts, S. Targan, S.B. Hanauer, L. Mayer, R.A. van Hogezand, D.K. Podolsky, B.E. Sands, T. Braakman, K.L. DeWoody, T.F. Schaible, S.J. van

Deventer, Infliximab for the treatment of fistulas in patients with Crohn's disease, N. Engl. J. Med. 340 (18) (1999) 1398–1405.
[44] S.B. Hanauer, B.G. Feagan, G.R. Lichtenstein, L.F. Mayer, S. Schreiber, J.F. Colombel, D. Rachmilewitz, D.C. Wolf, A. Olson, W. Bao, P. Rutgeerts, Maintenance infliximab for Crohn's disease: the ACCENT I randomised trial, Lancet 359 (9317) (2002) 1541–1549.
[45] C. Su, B.A. Salzberg, J.D. Lewis, J.J. Deren, A. Kornbluth, D.A. Katzka, R.B. Stein, D.R. Adler, G.R. Lichtenstein, Efficacy of anti-tumor necrosis factor therapy in patients with ulcerative colitis, Am. J. Gastroenterol. 97 (10) (2002) 2577–2584.
[46] L. de Ridder, J.C. Escher, J. Bouquet, J.J. Schweizer, E.H. Rings, J.J. Tolboom, R.H. Houwen, O.F. Norbruis, B.H. Derkx, J.A. Taminiau, Infliximab therapy in 30 patients with refractory pediatric crohn disease with and without fistulas in The Netherlands, J. Pediatr. Gastroenterol. Nutr. 39 (1) (2004) 46–52.
[47] P. Rutgeerts, G. Van Assche, S. Vermeire, Optimizing anti-TNF treatment in inflammatory bowel disease, Gastroenterology 126 (6) (2004) 1593–1610.
[48] T.N. Brooklyn, M.G. Dunnill, A. Shetty, J.J. Bowden, J.D. Williams, C.E. Griffiths, A. Forbes, R. Greenwood, C.S. Probert, Infliximab for the treatment of pyoderma gangrenosum: a randomised, double blind, placebo controlled trial, Gut 55 (4) (2006) 505–509.
[49] A Swaminath, S. Lichtiger, Dilation of colonic strictures by intralesional injection of infliximab in patients with Crohn's colitis, Inflamm. Bowel Dis. 14 (2) (2008) 213–216.
[50] D.M. Knight, H. Trinh, J. Le, S. Siegel, D. Shealy, M. McDonough, B. Scallon, M.A. Moore, J. Vilcek, P. Daddona, et al., Construction and initial characterization of a mouse–human chimeric anti-TNF antibody, Mol. Immunol. 30 (16) (1993) 1443–1453.
[51] B.J. Scallon, M.A. Moore, H. Trinh, D.M. Knight, J. Ghrayeb, Chimeric anti-TNF-alpha monoclonal antibody cA2 binds recombinant transmembrane TNF-alpha and activates immune effector functions, Cytokine 7 (3) (1995) 251–259.
[52] S.A. Siegel, D.J. Shealy, M.T. Nakada, J. Le, D.S. Woulfe, L. Probert, G. Kollias, J. Ghrayeb, J. Vilcek, P.E. Daddona, The mouse/human chimeric monoclonal antibody cA2 neutralizes TNF in vitro and protects transgenic mice from cachexia and TNF lethality in vivo, Cytokine 7 (1) (1995) 15–25.

iPS細胞のエピゲノム

——再生医療に向けたiPS細胞のクオリティコントロールにおけるエピゲノム解析の有用性

Epigenetics in iPS cells

山田泰広(写真)　山中伸弥

Yasuhiro YAMADA[1,2] and Shinya YAMANAKA[1]

京都大学 iPS 細胞研究所[1]，科学技術振興機構さきがけ[2]

◎iPS 細胞(induced pluripotent stem cell)はすべての体細胞に分化しうるという点で，再生医療のソースとして大きな期待を集めている．しかし，樹立された iPS 細胞の性質にはライン間でのバリエーションが存在することが明らかとなり，再生医療の実現のために，均一で質の高い iPS 細胞の作製や，iPS 細胞の個性に準じた応用方法の開発が望まれている．近年，エピジェネティック修飾状態の差異が iPS 細胞の質に変化を及ぼしうることが明らかとなりつつある．再生医療に有用な iPS 細胞の樹立・選別のためには，iPS 細胞におけるエピゲノム解析およびエピゲノム制御機構の理解が非常に重要な課題となると考えられる．本稿では iPS 細胞のエピゲノム制御について最新の知見を紹介し，それらの知見を背景とした iPS 細胞の再生医療に向けた応用の可能性について議論したい．

Key word　iPS細胞，再生医療，疾患特異的 iPS 細胞

分化した体細胞に 4 つの異なる転写因子を導入することで，胚性幹細胞(ES 細胞)とほぼ同等の細胞，すなわち induced pluripotent stem cell(iPS 細胞)の樹立が可能となった[1,2]．iPS 細胞樹立の過程はエピジェネティック修飾状態の大きな改変を伴い，エピゲノムのリセットが重要な役割を果たすことが明らかとなりつつある．iPS 細胞はすべての体細胞に分化しうるという点で，再生医療のソースとして大きな期待を集めている．しかし一方で，樹立された iPS 細胞の性質には細胞株間でのバリエーションが存在することが明らかとなり，再生医療の実現のために，均一で質の高い iPS 細胞の作製や，iPS 細胞の個性に準じた応用方法の開発が望まれている．iPS 細胞のクオリティや個性はエピジェネティック修飾状態の差異に由来する可能性が考えられ，再生医療に有用な iPS 細胞の樹立・選別のためには，iPS 細胞におけるエピゲノム解析およびエピゲノム制御機構の理解が重要な課題となるであろう．

本稿では ES 細胞，iPS 細胞をはじめとする多能性幹細胞のエピゲノム制御について最新の知見を紹介し，それらの知見を背景とした iPS 細胞の再

サイドメモ　疾患特異的iPS細胞

多くの疾患において，疾患発症に関与する遺伝子の配列異常や SNP の違いが報告されている．遺伝的背景が発症に関与した疾患において iPS 細胞(疾患特異的 iPS 細胞)を樹立することで，病態解明や治療法開発をめざす試みがなされている．さまざまな疾患特異的 iPS 細胞を作製し，それぞれの疾患において原因となる機能性体細胞へ分化誘導させることで，疾患のモデル細胞を作製しようとする研究が盛んに行われている．iPS 細胞は患者自身の体細胞から樹立でき，疾患原因細胞への分化誘導が可能であるのみならず，無限に細胞供給できることは，疾患特異的 iPS 細胞を用いた研究において大きな利点となりうる．このように，iPS 細胞は再生医療のソースとしての応用が注目されているのみならず，病態解明や新規治療方法の開発におけるツールとしても大きな期待が寄せられている．

生医療への応用の可能性について議論したい．

ES細胞のエピゲノム

ES細胞(embryonic stem cell)は胚盤胞の内部細胞塊から樹立される細胞で，個体すべての細胞に分化しうる多能性を有している一方で，無限の細胞増殖能をもちあわせている．ES細胞のDNA一次配列は基本的に分化細胞と同一であることから，ES細胞の多能性維持，分化の制御には転写因子による制御と密接に関連したエピゲノムのコントロールが重要な役割を果たしていることが予想される．ES細胞の多能性維持には，Oct3/4, Nanog, Sox2の転写因子によるコアネットワークの活性化が必須であることが示され，転写因子の重要性が強調されてきた[3]．

一方で，DNAメチル化やヒストン修飾などのエピジェネティック修飾状態変化を誘導するエピゲノム制御がどのようにしてES細胞の多能性を維持しているのか，一方で複数の細胞系譜への分化を許容するフレキシブルな状態を維持しているのかについては，いまだ不明な点が多い．次世代高速シークエンサーをはじめとする解析技術の進歩により，ES細胞におけるゲノム網羅的なエピゲノム解析が行われ，多能性細胞に特徴的ないくつかのエピジェネティック修飾状態およびエピゲノム制御機構が明らかになりつつある．

DNAメチル化

シトシンのメチル化は遺伝子発現制御，個体発生，各種疾患に重要な役割を果たすことが示されており，エピゲノム制御の中心的存在のひとつとなっている[4]．DNAのメチル化はサイレントなクロマチン状態と相関があり，一般にプロモーター領域のDNAメチル化はその遺伝子発現量とは負の相関がみられる．メチル化シトシンに対する抗体，メチル化DNA結合ドメイン(MBD)やメチル化感受性制限酵素などと次世代高速シークエンサーを組み合わせた方法により，ES細胞におけるゲノムスケールでのDNAメチル化マップが作成された．

以前から哺乳類シトシンのメチル化はCpG配列のシトシンに存在すると考えられてきた．しかし，ヒトES細胞においては約1/4のメチル化シトシンは非CpG配列(CNGおよびCNN)にみられることが最近報告された[5]．ヒト分化細胞ではほぼすべてのメチル化シトシンがCpG配列に検出されることから，非CpG配列のシトシンメチル化はES細胞特異的な現象と考えられ，機能的な意義解明が待たれる．

ヒストン修飾およびヒストンバリアント

ヒストンの60種類以上の残基にメチル化，アセチル化，リン酸化などによるさまざまな化学的修飾が観察される．DNAメチル化マップと同様にして，修飾ヒストンに対する抗体により濃縮されたヌクレオソームからのDNA断片を次世代シークエンサーで同定することによりゲノムスケールでのヒストン修飾パターンが明らかとなってきた．転写活性化領域にはヒストンH4のアセチル化，H3の4番目のリジン(H3K4)のメチル化がしばしば観察され，反対に転写不活性化領域にはH3K9メチル化，H3K27のメチル化が濃縮されている．ES細胞においては，細胞分化に重要な遺伝子は転写活性化マークのH3K4メチル化と不活性化マークであるH3K27メチル化が同時に存在する“bivalent domain”を形成し，転写が抑制されている[6]．ES細胞の分化によりbivalent domainにおけるH3K27メチル化が解除されることにより，H3K4メチル化単独のunivalent domainへと変化するとともに，速やかに転写が活性化される．DNA脱メチル化酵素の有無についての議論がはじまって久しいが，DNAメチル化は安定したエピジェネティック修飾であることを考えると，ES細胞/iPS細胞における遺伝子発現制御のフレキシビリティーとしてbivalent domainをはじめとするヒストン修飾状態が重要な役割を果たしていることが想像される．

ヒストンの修飾に加えてヒストンそのものにおけるバリアントの存在が知られる．そのなかでもH2AZはES細胞において転写不活性化因子であるポリコーム群複合体の標的部位に濃縮されており，機能的にも転写に抑制的に働いていることが示された．未分化性維持，細胞分化の制御にはヌクレオソームにおけるヒストンバリアントの使い

分けも関与していることが明らかとなりつつある[7]．

多能性幹細胞分化に伴うエピゲノムの変化

細胞分化に伴い，エピゲノムが変化することが予想されてきたものの，具体的な変化に関しての情報はいまだ乏しい．Meissnerらは ES 細胞と神経幹細胞の DNA メチル化状態をゲノム網羅的に解析し，ヒストン修飾状態と比較検討した[8]．その結果，予想されていたように，DNA メチル化状態は細胞の分化により大きく変化することが確認された．

注目すべきは，細胞分化によって DNA メチル化状態が変化する領域は highly conserved non-coding element とよばれる領域に顕著であり，いままで注目されてきた CpG island が存在するコアプロモーター領域では大きな変化が少ないことであった．さらに，ES 細胞と神経幹細胞の DNA メチル化状態の比較により，基本的に DNA メチル化レベルは CpG 配列の密度に反比例する傾向がみられるが，その例外もしばしば観察されることが明らかになった．その反面，DNA メチル化の変化はヒストンの修飾パターンの変化と非常によく相関することが示された．この現象は DNA メチル化パターンの形成は DNA の一次配列に依存しているというよりも，エピジェネティック修飾状態自身により決定されることを示唆している．これら Meissner らの仕事のなかで，神経幹細胞由来アストロサイトを試験管内で培養し継代を繰り返すと，CpG 密度の高い領域において異常な DNA メチル化が出現しはじめることが示された．このことは培養細胞を用いたエピジェネティック修飾状態の解析に対して警鐘を鳴らすとともに，癌細胞における CpG island の異常メチル化の由来を示唆する結果と考えられ，意義深い．

iPS細胞の樹立とリプログラミングによるエピゲノムの変化

2006 年，分化したマウス体細胞に 4 つの転写因子，Oct3/4，Sox2，Klf4，Myc を導入することで，多能性をもった iPS 細胞の樹立が可能となった[2]．2007 年には，ヒト細胞においても iPS 細胞の樹立が可能となり[1]，現在再生医療への応用に向けた取組みがなされている[9,10]．iPS 細胞の樹立のメカニズムはいまだ不明な点が多い．すくなくとも，iPS 細胞の樹立には週単位の時間を必要とする一方で，4 因子が導入されても大部分の細胞はリプログラミングに失敗することが明らかになっている．より効率的なリプログラミング法開発，そして再生医療を念頭においた安全なリプログラミング法開発のためには，リプログラミング過程の詳細な理解が必要と考えられる．

iPS 細胞は ES 細胞に類似した形態，生物学的特徴を示すのみならず，iPS 細胞のエピジェネティック修飾状態は ES 細胞の修飾状態に類似していることが示された．すなわち，リプログラミング過程では分化細胞のエピジェネティック修飾パターンから ES 細胞のパターンへと大きく変化する．実際に，マウス iPS 細胞でのヒストン修飾状態は ES 細胞に類似したパターンを有し，X 染色体の再活性化も確認されているし[11]，ヒト iPS 細胞とヒト ES 細胞のヒストン修飾状態に明らかな違いがないことが報告されている．したがって，エピジェネティック修飾状態の改変がリプログラミングの重要なイベントであることが予想されている．

以前から分化細胞の核は脱核した卵子への核移植，および embryonal carcinoma 細胞(EC 細胞)/ES 細胞との細胞融合によってリプログラミングされることが示されてきた[12-14]．iPS 細胞の樹立には週単位の時間が必要であるのに対して，核移植によるリプログラミングは 1〜2 日以内に，しかもわずか 1〜2 回の細胞分裂の間に速やかに誘導され，リプログラミングに要する時間がまったく異なる．すなわち，iPS 細胞樹立と核移植はリプログラミング経路が異なることが示唆される．

この 2 つのリプログラミング過程の違いを説明しうるひとつの因子は DNA 脱メチル化反応と考えられる[15]．DNA メチル化は DNA 合成に際して，おもに DNA methyltransferase 1(DNMT1)により安定的に維持されることがわかっている．一方で，一度付加されたシトシンのメチル基がはずれる，すなわち脱メチル化反応については 2 つの異なる系が提唱されている．ひとつは受動的な脱メチル

化反応で，DNA 複製の際に，メチル基を新規合成 DNA 鎖に付加せず，結果的にメチル化レベルが低下する系である．他方は能動的脱メチル化反応である．受精直後の雄性核は速やかに DNA メチル化レベルが低下することが観察されている．このメチル化レベルの低下には新規 DNA 合成は伴っておらず，初期の受精卵には積極的に DNA メチル化を解除する機構が存在することが示唆されている．

近年，AID/Mbd4/Gadd45a による deamination, glycosylation を介した脱メチル化反応のメカニズムが提唱されている[16,17]．体細胞においては明らかな能動的 DNA 脱メチル化反応は証明されておらず，能動的脱メチル化反応は受精卵などの特殊な細胞における特異的な反応であることが示唆されている．ES 細胞との細胞融合によるリプログラミングにおいては *Nanog* locus の DNA 脱メチル化は DNA 複製を伴わず，わずか 1 日の間に観察され，iPS 細胞樹立の過程と比べると非常に短時間で DNA 脱メチル化反応が生じることから，能動的 DNA 脱メチル化反応の関与が予想されている．

一方で，体細胞に転写因子を導入する iPS 細胞樹立の過程では *Nanog* locus などの DNA 脱メチル化は late event であり，核移植，細胞融合における脱メチル化に比べて長い時間を要することが示されている．体細胞において能動的 DNA 脱メチル化反応が存在しないとすれば，能動的脱メチル化反応の有無がリプログラミングに要する時間を規定している可能性がある．実際に AID の発現を低下させた ES 細胞との細胞融合によるリプログラミングにおいて，AID が DNA 脱メチル化反応および *OCT3/4* や *NANOG* の活性化に必要であることが示され，すくなくとも細胞融合によるリプログラミングには AID を介した能動的 DNA 脱メチル化反応が関与していることが示唆されている[17]．

以上から，能動的 DNA 脱メチル化反応の積極的な誘導が可能であれば，iPS 細胞樹立過程において樹立効率の向上，スピード促進が期待されるのみならず，iPS 細胞の質の向上にもつながる可能性が考えられる．まずは能動的脱メチル化反応のメカニズム解明が重要であろう．AID/Mbd4/Gadd 45a による脱メチル化反応に加えて，Tet による水酸化メチル化シトシンへの変換を介したシトシン脱メチル化反応の可能性が提唱されている．実際に Tet は ES 細胞未分化性維持機構への関与が報告されており[18]，今後の研究の展開が期待される．

iPS細胞とES細胞とのエピゲノム比較

前述のように iPS 細胞は ES 細胞に類似した遺伝子発現パターンを示すのみならず，ヒストンの修飾パターン，DNA メチル化状態などのエピジェネティック修飾状態においても ES 細胞とほぼ同一の特徴を有している．しかし，iPS 細胞が胚盤胞内部細胞塊由来の ES 細胞と完全に同一の性質を有するかどうかについては議論が続いている．実際に，多くのマウス iPS 細胞は ES 細胞に比べてキメラマウスにおけるキメラ寄与率が低いことが知られ，tetraploid complementation assay においては，ほとんどのマウス iPS 細胞では全身が iPS 細胞に由来するマウスは作製できないことが知られてきた．最近，一部のマウス iPS 細胞においては *Dlk1-Dio3* 遺伝子インプリント領域における遺伝子発現が ES 細胞と比べて抑制されていることが報告された[19]．興味深いことに，*Dlk1-Dio3* 遺伝子領域の発現低下を伴う iPS 細胞では，*Dlk1-Dio3* 遺伝子領域の DMR(differentially methylated region)の DNA メチル化パターンの異常がみられ，iPS 細胞からのマウス形成能にも影響が観察されるという．エピジェネティック修飾状態の違いが iPS 細胞の性質を変化させうることを示唆しているかもしれない．今後，これらが普遍的に iPS 細胞全体に適応されるのかを慎重に検証する必要がある．

iPS細胞の由来による性質の違い

異なる細胞から樹立された iPS 細胞はその由来細胞へ分化しやすいことが報告された[20,21]．たとえば，血液由来の iPS 細胞は血液に分化しやすく，間葉系由来の iPS 細胞はより骨に分化しやすい性質を有する．さらには異なる細胞から樹立された iPS 細胞は，DNA メチル化修飾パターンの違いか

ら区別しうることが報告された．すなわち，iPS細胞には由来する細胞の epigenetic memory が存在することが示唆された．Epigenetic memory の存在を検証し理解するためには，iPS細胞の分化指向性と具体的な DNA メチル化状態の差異との関連を明らかする必要があるであろう．興味深いことに，核移植によりリプログラミングされた ntES細胞の DNA メチル化状態は iPS 細胞に比べて，より ES 細胞に近いことが報告された．核移植によるリプログラミングがより効率的にエピジェネティック修飾状態を改変しうる可能性を示している．

上述したように，DNA メチル化はより安定的で“deep”なサイレンシングに関与していると考えられており，核移植後の卵子に存在する能動的 DNA 脱メチル化反応の存在が，効率的な DNA メチル化状態改変に重要な役割を果たしているのかもしれない．

再生医療に向けたiPS細胞のクオリティコントロールとエピゲノム

再生医療に使用する iPS 細胞のクオリティーコントロールの観点から，iPS 細胞株間での分化指向性の違いや，由来細胞に依存した iPS 細胞株間の DNA メチル化修飾状態の違いは iPS 細胞の質のバリエーションを示唆するものであり，均一な iPS 細胞を選別するためにはエピゲノム解析が有用と考えられる．しかし，エピゲノムの違いがどのように，そしてどの程度 iPS 細胞の質に影響を与えるのかはいまだ不明である．

今後は iPS 細胞の詳細なエピゲノム解析に加えて，細胞分化を規定するエピゲノム制御機構の理解を深めることが重要と考えられる．エピジェネティック修飾状態は DNA 脱メチル化剤やヒストン脱アセチル化酵素阻害剤などの処理により変化させうることが示唆されており，エピジェネティック修飾薬剤の利用および新規開発は質の高い均一な iPS 細胞を得るためのアプローチとなりうるであろう．iPS 細胞は再生医療への応用において期待されているのみならず，疾患特異的 iPS 細胞を用いた病態解析において非常に有用なツールとなっている．疾患特異的 iPS 細胞の性質を評価する場合には，iPS 細胞自体におけるエピジェネティック修飾状態のばらつきの存在を念頭におき，疾患本来の表現形との明確な区別をすることが重要となるであろう．一方で，エピジェネティック修飾状態の差異は iPS 細胞の個性ととらえることもできる．効率的な機能性分化細胞の誘導のために，エピジェネティック修飾状態の違いに由来する iPS 細胞の個性を積極的に利用するアプローチが有効かもしれない．

文献

1) Takahashi, K. et al.：Induction of pluripotent stem cells from adult human fibroblasts by defined factors. *Cell*, **131**：861-872, 2007.
2) Takahashi, K. and Yamanaka, S.：Induction of pluripotent stem cells from mouse embryonic and adult fibroblast cultures by defined factors. *Cell*, **126**：663-676, 2006.
3) Niwa, H.：How is pluripotency determined and maintained? *Development*, **134**：635-646, 2007.
4) Jaenisch, R. and Bird, A.：Epigenetic regulation of gene expression：how the genome integrates intrinsic and environmental signals. *Nat. Genet.*, **33**(Suppl.)：245-254, 2003.
5) Lister, R. et al.：Human DNA methylomes at base resolution show widespread epigenomic differences. *Nature*, **462**：315-322, 2009.
6) Bernstein, B. E. et al.：A bivalent chromatin structure marks key developmental genes in embryonic stem cells. *Cell*, **125**：315-326, 2006.
7) Creyghton, M. P. et al.：H2AZ is enriched at polycomb complex target genes in ES cells and is necessary for lineage commitment. *Cell*, **135**：649-661, 2008.
8) Meissner, A. et al.：Genome-scale DNA methylation maps of pluripotent and differentiated cells. *Nature*, **454**：766-770, 2008.
9) Okita, K. et al.：Generation of mouse-induced pluripotent stem cells with plasmid vectors. *Nat. Protoc.*, **5**：418-428, 2010.
10) Nakagawa, M. et al.：Promotion of direct reprogramming by transformation-deficient Myc. *Proc. Natl. Acad. Sci. USA*, **107**：14152-14157, 2010.
11) Maherali, N. et al.：Directly reprogrammed fibroblasts show global epigenetic remodeling and widespread tissue contribution. *Cell Stem Cell*, **1**：55-70, 2007.
12) Gurdon, J.：Nuclear reprogramming in eggs. *Nat. Med.*, **15**：1141-1144, 2009.
13) Wilmut, I. et al.：Viable offspring derived from fetal and adult mammalian cells. *Nature*, **385**：810-813, 1997.
14) Miller, R. A. and Ruddle, F. H.：Pluripotent teratocarcinoma-thymus somatic cell hybrids. *Cell*, **9**：45-55, 1976.
15) Yamanaka, S. and Blau, H. M.：Nuclear reprogramming to a pluripotent state by three approaches.

Nature, **465**：704-712, 2010.
16) Rai, K. et al.：DNA demethylation in zebrafish involves the coupling of a deaminase, a glycosylase, and gadd45. *Cell*, **135**：1201-1212, 2008.
17) Bhutani, N. et al.：Reprogramming towards pluripotency requires AID-dependent DNA demethylation. *Nature*, **463**：1042-1047, 2010.
18) Ito, S. et al.：Role of Tet proteins in 5mC to 5hmC conversion, ES-cell self-renewal and inner cell mass specification. *Nature*, **466**：1129-1133, 2010.
19) Stadtfeld, M. et al.：Aberrant silencing of imprinted genes on chromosome 12qF1 in mouse induced pluripotent stem cells. *Nature*, **465**：175-181, 2010.
20) Kim, K. et al.：Epigenetic memory in induced pluripotent stem cells. *Nature*, **467**：285-290, 2010.
21) Polo, J. M. et al.：Cell type of origin influences the molecular and functional properties of mouse induced pluripotent stem cells. *Nat. Biotechnol.*, **28**：848-855, 2010.

*　　*　　*

＊＊次号の特集予告(235巻11号)＊＊＊＊＊＊＊＊＊＊＊＊＊＊＊＊＊＊＊＊＊＊＊＊＊＊＊＊＊＊＊＊＊＊

◆動き出した“エコチル調査”

――環境省「子どもの健康と環境に関する全国調査」

(企画：佐藤　洋／東北大学大学院医学系研究科環境保健医学分野)

＊＊

エコチル調査は10万人の出生児を対象とし，その両親も加えると30万人と大規模である．リクルート期間は3年，出生児が13歳になるまで追跡調査し，さらに解析期間も含めると20年余にわたる．胎児期を中心とする小児期化学物質曝露の発育・発達への影響を明らかにすることが調査の主目的であるが，その他の環境要因や遺伝要因の影響も明らかにしないと，化学物質の真の影響は解明されない．発育・発達の“正常値”も明らかになろう．したがって，子どもの発育・発達に関する包括的な調査研究になり，その成果への期待も大きい．研究計画はさらに磨きをかけていかなければならず，この出生コホート調査が子どもとともに育っていくことを期待する．本特集では，このような調査に至るまでの経緯や，これからはじまる調査への期待なども含めて，この調査の立ち上げに努力してきた先生方，これから調査を実施していく先生方に，その概要を紹介いただく．

CD13 is a therapeutic target in human liver cancer stem cells

Naotsugu Haraguchi,[1,2] Hideshi Ishii,[1,3] Koshi Mimori,[3] Fumiaki Tanaka,[3] Masahisa Ohkuma,[4] Ho Min Kim,[1] Hirofumi Akita,[1] Daisuke Takiuchi,[1] Hisanori Hatano,[1] Hiroaki Nagano,[1] Graham F. Barnard,[5] Yuichiro Doki,[1] and Masaki Mori[1]

[1]Department of Gastroenterological Surgery, Graduate School of Medicine, Osaka University, Osaka, Japan. [2]Excellent Young Researchers Overseas Visit Program, Japan Society for the Promotion of Science (JSPS), Tokyo, Japan. [3]Department of Surgery, Medical Institute of Bioregulation, Kyushu University, Oita, Japan. [4]Department of Surgery, Jikei University School of Medicine, Tokyo, Japan. [5]Department of Medicine, University of Massachusetts Medical School, Worcester, Massachusetts, USA.

Cancer stem cells (CSCs) are generally dormant or slowly cycling tumor cells that have the ability to reconstitute tumors. They are thought to be involved in tumor resistance to chemo/radiation therapy and tumor relapse and progression. However, neither their existence nor their identity within many cancers has been well defined. Here, we have demonstrated that CD13 is a marker for semiquiescent CSCs in human liver cancer cell lines and clinical samples and that targeting these cells might provide a way to treat this disease. CD13$^+$ cells predominated in the G_0 phase of the cell cycle and typically formed cellular clusters in cancer foci. Following treatment, these cells survived and were enriched along the fibrous capsule where liver cancers usually relapse. Mechanistically, CD13 reduced ROS-induced DNA damage after genotoxic chemo/radiation stress and protected cells from apoptosis. In mouse xenograft models, combination of a CD13 inhibitor and the genotoxic chemotherapeutic fluorouracil (5-FU) drastically reduced tumor volume compared with either agent alone. 5-FU inhibited CD90$^+$ proliferating CSCs, some of which produce CD13$^+$ semiquiescent CSCs, while CD13 inhibition suppressed the self-renewing and tumor-initiating ability of dormant CSCs. Therefore, combining a CD13 inhibitor with a ROS-inducing chemo/radiation therapy may improve the treatment of liver cancer.

Introduction

Functional and morphologic heterogeneity exists in a tumor with a hierarchy in which tumor growth is driven by a small subset of cancer stem cells (CSCs) (1). Like normal tissue stem cells, which are capable of self renewal and multidifferentiation, CSCs have the ability to reconstitute tumors (2). In the hematologic cell lineage, stem cells exist in the dormant phase and can be detected as a side population (SP) (3). Generally, CSCs, like somatic tissue stem cells, proliferate slowly, i.e., they are in the dormant or slow-growing phase of the cell cycle. This partially accounts for their therapeutic refractoriness to chemo/radiation therapy, tumor relapse, and presumably metastasis. The CSCs of acute myeloid leukemia (4) and chronic myeloid leukemia (5) also survive in the dormant G_0 phase of the cell cycle in a bone marrow niche after chemotherapy. Relapses and metastases of breast cancer often occur after intervals of several decades, suggesting the involvement of a deep dormant phase for CSCs (6). The majority of liver cancers are superimposed on a background of chronic hepatitis and hepatic cirrhosis. Therefore, it may be difficult to distinguish between intrahepatic metastasis through portal or hepatic venules and metachronous multicentric development of liver cancer in a precancerous background. However, there are some cases of liver cancer in which cancer recurs in the liver or metastasizes to the lung and bone several years after radical hepatectomy or liver transplantation. This suggests that some slow-growing cancer cells also exist in liver cancer but these may not be in deep dormancy like breast cancer CSCs.

Anticancer reagents in clinical use generally affect division and proliferation of cancer cells. This could result in elimination of proliferating cancer cells but not reduce the survival of CSCs in the dormant or slow-growing phase. Thus, the identification and characterization of dormant or slow-growing CSCs are important for developing novel therapeutic approaches.

In studies of hepatocellular carcinoma (HCC) (7), the fifth most common cancer in the world, the SP fraction (8), CD133$^+$ (9–11), CD44$^+$ (11, 12), CD90$^+$ (12, 13), and epithelial cell adhesion molecules (14) were reported as markers of CSCs or cancer-/tumor-initiating cells. The majority of CSC studies focus on identification of cell markers to enrich cell populations that have high tumor initiation ability in immune-deficient mice. In the field of liver cancer CSCs, there have been few reports describing dormant or slow-growing CSCs that include their cellular characteristics or indicate a way to target these cells based on cytological evidence. In addition, there have been few reports that clearly indicate the interrelationships among these candidate markers.

In a previous study (similar to hematopoietic and leukemic studies), we reported that the SP fraction enriches the CSC-like fractions. Cells of the SP fraction express both hepatocyte and cholangiocyte markers, show high resistance to anti-cancer agents, and high tumorigenicity in NOD/SCID mice (8). Based on our previous data (8) and applying the techniques of hematopoietic stem cell studies (3–5), our aims were as follows: first, to clarify the relationships between reported candidate CSC markers; second, to assess whether dormant CSCs exist in liver cancer and to concentrate on cell-surface markers, which definitively identify potentially dormant CSCs; third, to clarify the cellular characteristics of potentially dormant CSCs and to identify the mechanisms that protect potentially dormant CSCs from chemo/radiation therapy; finally, to identify target molecules of liver cancer CSCs to initiate novel approaches that could lead to a future radical cure for liver cancer.

Conflict of interest: The authors have declared that no conflict of interest exists.
Citation for this article: *J Clin Invest.* 2010;120(9):3326–3339. doi:10.1172/JCI42550.

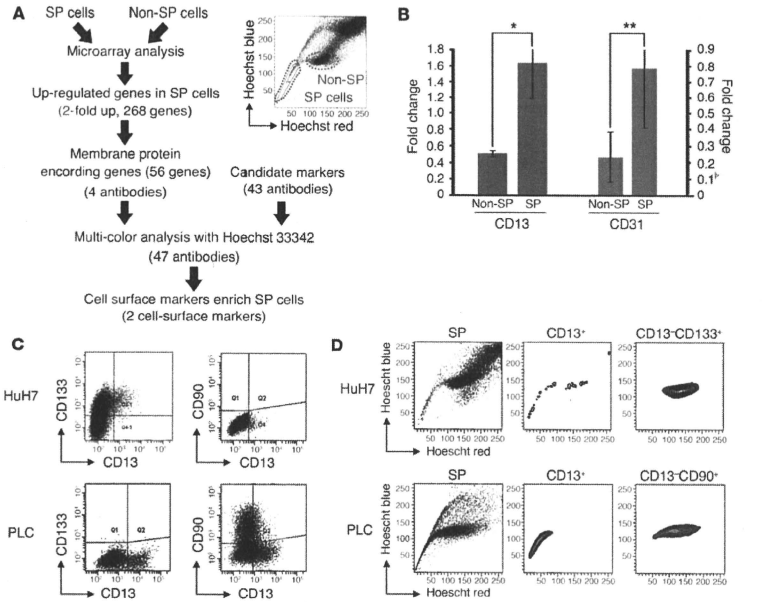

Figure 1

CD13 is a candidate marker of the SP fraction. **(A)** The strategy used to identify cell-surface markers closely related to the SP fraction. We determined CD13 and CD31 as candidate markers for identifying SP cells. **(B)** Both CD13 and CD31 expression in HuH7 cells were compared in SP and non-SP cells by semiquantitative RT-PCR. Data represent mean ± SD from independent experiments of fractions differentially sorted by flow cytometry. $^*P < 0.01$; $^{**}P = 0.076$ versus non-SP fractions. The cut-off lines were determined using isotype controls. **(C)** Expression of CD13, CD133, and CD90 in HuH7 (upper panels) and PLC/PRF/5 cells (lower panels). Horizontal and vertical axes denote expression intensity. **(D)** The SP fraction is recognized as a "beak" appearing beside the G_1 phase fraction. The relationship between $CD13^+$ and $CD13^-$ cells and the SP fraction was studied using multicolor flow cytometry.

Results

CD13 is a candidate marker closely correlated with SP cells. To identify specific cell-surface markers that correlate with the SP fraction, we utilized our previous data sets of SP and non-SP fraction gene expression profiles obtained using microarray analyses (8). From a list of 268 genes upregulated in the SP cells (with a fold change > 2) (8), we selected 56 genes that potentially encode cell-surface proteins via the UniProtKB database (http://www.uniprot.org/). Working from the list of 56 upregulated genes (Supplemental Table 1; supplemental material available online with this article; doi:10.1172/JCI42550DS1) and an additional 43 markers reported to be closely associated with normal stem cells and CSCs, we tested 47 commercially available antibodies (Supplemental Table 2) to identify surface markers that were enriched in the SP fraction (Figure 1A).

During this screening, we identified 2 candidate markers, CD13 and CD31. The expression analysis of CD13 was 1.64 ± 0.45 in the SP and 0.51 ± 0.03 in the non-SP cell fraction ($P < 0.01$) (Figure 1B). We focused on CD13 in the current study, since the expression of CD31 was abundant in the G_2/M/SP fraction but was not universal in the liver cancer cell lines studied by us (HuH7, PLC/PRF/5, and Hep3B), and the statistical significance was weak ($P = 0.076$) (Figure 1B and Supplemental Figure 1, A and B).

Expression of CD13, CD133, and CD90 was assessed in hepatitis infection–negative (HuH7) and –positive (PLC/PRF/5) cell lines. The expression of CD133 was detected in HuH7 but not in PLC/PRF/5, and the expression of CD90 was detected in PLC/PRF/5 but not in HuH7. The expression of CD13 was observed in both these cell lines as well as in Hep3B (Figure 1C and Supplemental Figure 1A). In HuH7 in particular, the $CD13^+$ cells typically existed in a $CD133^{strong}$ fraction ($CD13^+CD133^+$).

Multicolor analysis with Hoechst staining exhibited clear localization of $CD13^+$ cells in the SP fraction of HuH7 and PLC/PRF/5, whereas the $CD13^-CD133^+$ and $CD90^+$ fractions were localized to the G_1-to-G_2 fraction and not the SP fraction (Figure 1D). To confirm the cell-cycle status of the $CD13^+$ cells in PLC/PRF/5, cell-cycle analysis by combined multicolor analysis and 7-amino-actinomy-

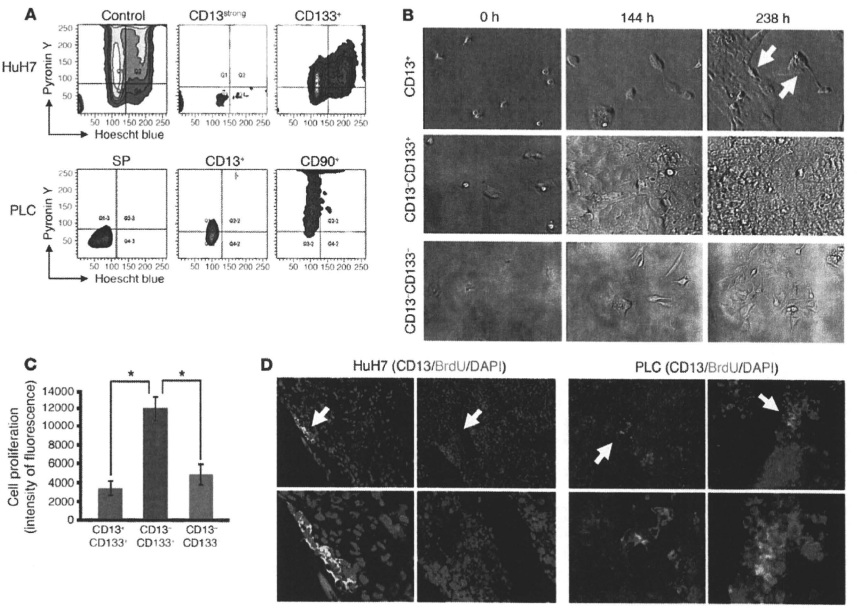

Figure 2

CD13 is a candidate marker of dormant to slow-growing CSCs. (**A**) Dormant cells can be identified using the DNA-binding dye Hoechst 33342 and RNA-binding dye PY. Dormant cells contain lower RNA levels than G_1 phase cells. Combination analysis of the cell cycle with cell-surface markers CD13, CD133, and CD90 was performed with reserpine. The cut-off lines were determined using isotype controls. (**B**) Time-lapse cell-fate tracing of HuH7 cells. Cells were labeled with PKH26GL, isolated to their $CD13^+$, $CD13^-CD133^+$, and $CD13^-CD133^-$ fractions, and traced for 238 hours. The dye-retaining cells can be identified as red-labeled cells (white arrow). Original magnification, ×20. (**C**) Proliferation assay of the $CD13^+CD133^+$, $CD13^-CD133^+$, and $CD13^-CD133^-$ fractions. Data represent mean ± SD from independent experiments of fractions differentially sorted by flow cytometry. $^*P < 0.05$. (**D**) BrdU-retaining cells in serially transplanted control tumor specimens of HuH7 (6 weeks after BrdU injection) and PLC/PRF/5 (10 weeks after BrdU injection). The sections were stained with anti-CD13 (red), BrdU (green), and DAPI (blue). Top panels show lower magnification of the sections of HuH7 and PLC/PRF/5 (×10, HuH7 and left panel of PLC; ×20, right panel of PLC). The lower panels show high magnification (×40) of the place indicated by white arrows in the top panels.

cin D (7-AAD) DNA labeling was performed. The $CD13^+CD90^-$ population was mainly in the G_0/G_1 phase, and the $CD13^+CD90^+$ population was clearly in the S to G_2/M phase. The $CD13^-CD90^+$ cells were present in all phases of the cell cycle but were more clearly present in the G_2/M and S phases when compared with the $CD13^+CD90^-$ population (Supplemental Figure 1C).

In these studies, we confirmed CD13 as a universal candidate marker that correlates with the liver cancer SP fraction. There were no definitive single markers that showed a stronger correlation to the SP fraction than CD13 and, to a lesser extent, CD31.

CD13 is a marker of tumor-initiating and potentially dormant HCC cells. Given that hematopoietic and leukemic stem cells are in the G_0 phase, identification and characterization of dormant or slow-growing cancer cell populations is very important because of these populations' relevance to chemo resistance and recurrence. Studies of CD13 expression in HuH7 and PLC/PRF/5 and their relationships with the cell-cycle phase, using the DNA-binding dye Hoechst 33342 and the RNA-binding dye pyronin Y (PY) (3), indicated that most of the $CD13^+$ fraction exists in the G_1/G_0 phase and the $CD13^{strong}$ population was clearly localized in G_0. The $CD133^+$ population in HuH7 and the $CD90^+$ fraction in PLC/PRF/5 were distributed in the G_1/G_0 and G_2/M phases, respectively. The relationships between the SP fraction and the G_0 cell-cycle phase were also confirmed, and the SP fraction was clearly localized in the G_0 phase under reserpine-free (ABC transporter blocker) conditions (Figure 2A).

To study the cell fate and dye-retaining capacity of HuH7 $CD13^+$ cells, the cell-surface membrane was labeled with PKH26GL reagent and cell fate was traced for 238 hours. Equal numbers of cells were seeded for each population. The $CD13^+CD133^+$ fraction exhibited very slow growth compared with the $CD13^-CD133^+$ fraction, with the doubling time of the $CD13^+CD133^+$ fraction estimated

Table 1
Limiting dilution and serial transplantation assay of HuH7 and PLC/PRF/5 cells

Cell type	Assay	Marker/cells	1×10^2	5×10^2	1×10^3	5×10^3	1×10^4
HuH7	Limiting dilution	$CD13^+CD133^+$	2/4	2/4	3/4	3/4	–
HuH7	Limiting dilution	$CD13^-CD133^+$	0/4	0/4	3/4	4/4	–
HuH7	Limiting dilution	$CD13^-CD133^-$	0/4	0/4	0/4	0/4	–
HuH7	Serial transplantation	$CD13^+CD133^+$	0/4	1/4	3/4	4/4	3/4
HuH7	Serial transplantation	$CD13^-CD133^+$	0/4	0/4	0/4	0/4	1/4
HuH7	Serial transplantation	Control	0/4	0/6	0/6	0/6	2/6
PLC	Limiting dilution	$CD13^+CD90^-$	2/4	2/2	4/4	3/3	–
PLC	Limiting dilution	$CD13^-CD90^+$	0/4	2/2	4/4	3/3	–
PLC	Limiting dilution	$CD13^-CD90^-$	0/4	0/4	0/3	0/4	–
PLC	Serial transplantation	$CD13^+CD90^-$	0/4	2/4	3/4	3/4	3/4
PLC	Serial transplantation	$CD13^-CD90^+$	0/4	0/4	0/4	0/4	1/4
PLC	Serial transplantation	Control	0/6	0/6	0/6	1/6	2/6

at approximately 160 hours. Dye-retaining cells could be observed 238 hours after cell seeding only in the $CD13^+CD133^+$ fraction (Figure 2B and Supplemental Videos 1–3). The $CD13^-CD133^-$ fraction exhibited cell fragmentation and apoptotic changes during cell culture. To confirm CD13 expression in association with cell growth, we performed cell proliferation assays. Data from isolated HuH7 populations showed that $CD13^+CD133^+$ cells exhibited slow cell growth compared with $CD13^-CD133^+$ cells 72 hours after seeding (Figure 2C). The $CD13^-CD133^-$ population also grew slowly but maintained viability for a week, with difficulty, because of apoptosis.

Next, tumor-formation ability of each fraction was studied in HuH7 and PLC/PRF/5 cells. Limiting dilution analysis of HuH7 cells revealed that the $CD13^+CD133^+$ fraction formed tumors from 100 cells (2/4), the $CD13^-CD133^+$ fraction formed tumors from 1,000 cells (3/4), and the $CD13^-CD133^-$ fraction formed no tumors from 5,000 cells (0/4) in NOD/SCID mice after 4 weeks of observation. In PLC/PRF/5 cells, the $CD13^+CD90^-$ fraction formed tumors from 100 cells (2/4), and the $CD13^-CD90^+$ fraction formed tumors from 5,000 cells (2/2), whereas the $CD13^-CD90^-$ cells formed no tumors from 5,000 cells (0/4) in NOD/SCID mice after 6 weeks of observation (Table 1). To assess the tumor formation ability definitively, formed tumors were digested, and isolated $CD13^+CD133^+$ and $CD13^-CD133^+$ fractions of HuH7 and isolated $CD13^+CD90^-$ and $CD13^-CD90^+$ fractions of PLC/PRF/5 were serially transplanted to secondary NOD/SCID mice. As controls, non-isolated cell fractions of HuH7 and PLC/PRF/5 were also serially transplanted. Tumor formation ability of $CD13^+$ cells compared with that of $CD13^-$ cells in serial transplantation assay was demonstrated more clearly than that of limiting dilution assay. In HuH7, after 6 weeks of observation, the $CD13^+CD133^+$ fraction formed tumors from 500 cells (1/4), whereas the $CD13^-CD133^+$ fraction and control formed very small tumors only in 10,000 cells (1/4 in the $CD13^-CD133^+$ fraction, and 2/6 in control). In PLC/PRF/5, after 6 weeks of observation, the $CD13^+CD90^-$ formed tumors from 500 cells (2/4), and the control formed tumors from 5,000 cells (1/6), whereas the $CD13^-CD90^+$ fraction formed 1 very small tumor only in 10,000 cells (1/4) (Table 1).

To assess semiquiescent status of $CD13^+$ cells in vivo, BrdU-retaining status was studied. Tumors obtained from NOD/SCID mice xenografted with HuH7 and PLC/PRF/5 cells were digested to single cells and serially transplanted without isolation of cell-surface markers. BrdU was injected intraperitoneally. After 6 weeks for HuH7, and after 10 weeks for PLC/PRF/5, tumors were enucleated and sections were stained with anti-BrdU and anti-CD13 antibody. In the tumors derived from HuH7 cells, very small numbers of BrdU-retaining cells that also expressed CD13 were observed typically in the edge of tumor foci. BrdU-retaining cells were not observed in the tumor center. Tumors derived from PLC/PRF/5 cells grew more slowly than did those derived from HuH7 cells. BrdU-retaining cells could be identified and did express CD13. Interestingly, clusters of $CD13^+$BrdU$^-$ cells were observed close to $CD13^+BrdU^+$ cells, suggesting that they might be derived from the $CD13^+BrdU^+$ cells (Figure 2D).

HCC-$CD13^+$ cells form spheres and produce the $CD90^+$ phenotype. Sphere formation is a common characteristic of stem cells. To evaluate CD13 as a candidate CSC marker, the expression of CD13 in spheres derived from HuH7, PLC/PRF/5, and clinical HCC was studied. The expression of CD13 was increased in both HuH7 (2.0% in control vs. 67.0% in spheres; 33.5-fold increase) and PLC/PRF/5 (15.2% in control vs. 83.8% in spheres; 5.51-fold increase) (Figure 3A). There was no significant change in CD133 expression in HuH7. In PLC/PRF/5, expression of CD90 was decreased in the spheres (35.7% in control vs. 2.5% in spheres; 14.28-fold decrease). The expression of CD13 compared with that of CD133 and CD90 appeared to be associated with a more immature stem-like and dormant population. Spheres established from clinical HCC samples localized in the $CD13^+CD90^-CD133^-$ fraction in a manner similar to that observed in PLC/PRF/5 (Figure 3B).

The time-course changes in the expression of CD13 and CD90 in PLC/PRF/5 were studied. Isolation and culture of the $CD13^+CD90^-$ fraction from the PLC/PRF/5 spheres in serum-containing media resulted in the production of $CD13^+CD90^+$ fraction after 96 hours (Figure 3C). The isolated $CD13^-CD90^-$ fraction elicited cell death within a few days and could not be maintained. Interestingly, the isolated $CD13^-CD90^+$ fraction rapidly produced the $CD13^+CD90^-$ fraction within 24 hours (Figure 3C). These findings suggest that potentially dormant $CD13^+$ cells produce proliferating $CD90^+$ cells and that some parts of the proliferating $CD90^+$ cells also produce $CD13^+$ cells. It is important to determine how this $CD13^+$ population (slow-growing potentially dormant) could be maintained in a cancer cell line in vitro. Dormant or slow-growing cell populations may disappear during continuous subculturing. These findings may replicate the rapid change from dormant to active status in cancer stem-like cells, as revealed by their cell-surface markers, or the dormant cells might mimic a certain multipotent condition in cellular differentiation.

$CD13^+$ cells resist chemotherapy, and CD13 inhibition drives cells to apoptosis. The change of cell-surface marker expression before and after doxorubicin (DXR) hydrochloride treatment or 5-fluorouracil (5-FU) was studied in HuH7 and PLC/PRF/5. In HuH7, CD13